

TOPICAL REVIEW

## Medical applications of magnetorheological fluid: a systematic review

To cite this article: Gaoyu Liu *et al* 2022 *Smart Mater. Struct.* **31** 043002

View the [article online](#) for updates and enhancements.

### You may also like

- [Development and damping properties of a seismic linear motion damper with MR fluid porous composite rotary brake](#)

Masami Nakano, Jian Yang, Shuaishuai Sun et al.

- [Active dispersing mechanism for settled magnetorheological fluid featuring with rotary blades and inductive coils in twin-tube damper](#)

Honghui Zhang, Zhiyuan Zou, Seung-Bok Choi et al.

- [Adaptive magnetorheological fluid energy absorption systems: a review](#)

Xianxu 'Frank' Bai, Xinchi Zhang, Young T Choi et al.



The banner features a blue background with circular ECS logos at the top and bottom. In the center, there's a photo of a smiling woman in a tan blazer. To her left, text details the meeting: "UNITED THROUGH SCIENCE & TECHNOLOGY", "The Electrochemical Society Advancing solid state & electrochemical science & technology", "248th ECS Meeting Chicago, IL October 12-16, 2025 Hilton Chicago". To her right, large text reads "Science + Technology + YOU!". At the bottom right, it says "SUBMIT ABSTRACTS by March 28, 2025". A red button at the bottom center says "SUBMIT NOW".

## Topical Review

# Medical applications of magnetorheological fluid: a systematic review

Gaoyu Liu<sup>1</sup> , Fei Gao<sup>2</sup> , Daihua Wang<sup>3,4</sup>  and Wei-Hsin Liao<sup>1,5,\*</sup> 

<sup>1</sup> Department of Mechanical and Automation Engineering, The Chinese University of Hong Kong, Shatin, Hong Kong, People's Republic of China

<sup>2</sup> Guangdong Provincial Key Lab of Robotics and Intelligent System, Shenzhen Institute of Advanced Technology, Chinese Academy of Sciences, Shenzhen, Guangdong, People's Republic of China

<sup>3</sup> Key Laboratory of Optoelectronic Technology and Systems of Ministry of Education of China, Chongqing University, Chongqing, People's Republic of China

<sup>4</sup> Precision and Intelligence Laboratory, Department of Optoelectronic Engineering, Chongqing University, Chongqing, People's Republic of China

<sup>5</sup> Institute of Intelligent Design and Manufacturing, The Chinese University of Hong Kong, Shatin, Hong Kong, People's Republic of China

E-mail: [whliao@cuhk.edu.hk](mailto:whliao@cuhk.edu.hk)

Received 16 April 2021, revised 28 June 2021

Accepted for publication 13 February 2022

Published 1 March 2022



## Abstract

Magnetorheological (MR) fluid, whose rheological properties can be changed reversibly by applied magnetic field, offers superior capabilities and opportunities since its invention. The most crucial feature of MR fluid is its controllable and continuous yield stress. Taking this advantage, MR fluid is gaining popularity in various medical applications to meet their force/torque requirements. In this review article, progress of medical applications of MR fluid in the last two decades are systematically reviewed, mainly focused on six categories: lower limb prosthesis, exoskeleton, orthosis, rehabilitation device, haptic master, and tactile display. With MR fluid, natural and stable limb motions in lower limb prostheses, exoskeletons, and orthoses, flexible muscle trainings in rehabilitation devices, and high transparency and resolution haptic feedback can be realized. Relevant discussions and future perspectives are also provided.

Keywords: magnetorheological fluid, lower limb prosthesis, exoskeleton, orthosis, rehabilitation device, haptic master, tactile display

(Some figures may appear in colour only in the online journal)

## 1. Introduction

Magnetorheological (MR) fluid, a kind of smart material with magnetically controllable rheological properties, is gaining much attention and popularity since its invention by Rainbow in 1948 [1]. This kind of fluid exhibits both Newtonian

(fluid state) and non-Newtonian (semi-solid state) behaviors. Transformation from Newtonian to non-Newtonian states is realized by applying magnetic field, which increases its viscosity and generates considerable yield stress. Due to fast response, large force/torque capacity, low power consumption, and design simplicity and compactness, MR fluid offers outstanding capability and draws great interest in civil, industrial, military, and medical applications. Particularly, medical

\* Author to whom any correspondence should be addressed.

applications of MR fluid are emerging in the 21st century, featuring lower limb prosthesis, exoskeleton, orthosis, rehabilitation device, haptic master, and tactile display.

Because of diseases, accidents, and disasters, the number of people who are subjected to limb disabilities is dramatically increasing. Some of them even undergo lower limb amputation. Incomplete bodies not only lead to reduced mobility in their daily lives, but also cause psychological problems. Also due to limb disabilities, people with able body are experiencing muscle weakness, partial or full paralysis, and loss of assistance in their upper and lower extremities [2]. Up till now, the primary strategy for lower limb amputees is to wear lower limb prostheses that provide weight support and locomotion aid [3]. Able-body people with limb disabilities are usually suggested to wear exoskeletons or orthoses for motion assistance. They can also use rehabilitation devices to train their limb muscles after injuries.

Meanwhile, the last few decades are witnessing the growing popularity of robot surgery since the surgeon does not need to directly operate on the patient and it has higher precision, smaller incisions, shorter hospitalization and faster recovery time [4]. One of the important technologies in robot surgery is haptics. The purpose of haptic feedback (force and tactile) in robot surgery is to provide ‘transparency’, in which the surgeon does not feel as if he/she is operating a remote device, but rather that his/her own hands are contacting the patient [5].

Common actuation mechanisms of lower limb prostheses, exoskeletons, orthoses, rehabilitation devices include electrical motor, hydraulic actuation, pneumatic actuation, mechanical structures like series elastic actuator (SEA) and ball-screw mechanism, etc [2, 6]. These actuation mechanisms are often complex in design, hard to realize; and consume much energy, which may lead to instability issues. As for haptic feedback in robot surgery, normal feedback mechanisms include electrical motor, audio, graphics, vibrotactile display, tactile sensor arrays, etc [5, 7]. Although some prototypes based on these mechanisms have been made, they are still in infant stage with relatively low transparency and resolution.

In view of the drawbacks of the current actuation and feedback mechanisms, MR fluid is used to meet the force/torque requirements of various medical applications. With MR fluid, limb motions of users wearing lower limb prostheses, exoskeletons, and orthoses become more natural and stable; muscle trainings with rehabilitation devices are getting more flexible; haptic feedback in robot surgery can have higher transparency and resolution.

Oh and Choi [8] as well as Sohn *et al* [9] briefly enumerated some medical applications of MR fluid. However, their descriptions on lower limb prosthesis and orthosis are very brief and sketchy, major advances such as exoskeleton and rehabilitation devices are not included. These two papers also lack relevant categorization, summaries, discussions, and future perspectives. Up till now, there is no systematic review on the progress of MR fluid in medical applications during the last two decades, which is quite desirable. Therefore, in this review article, medical applications of MR fluid are systematically reviewed. The rest of the paper is organized as follows.

Basic working mechanisms and principles of MR fluid and MR actuator are introduced in section 2. Then, six categories of medical applications of MR fluid, i.e. lower limb prosthesis, exoskeleton, orthosis, rehabilitation device, haptic master, and tactile display, are respectively described in sections 3–8. In each category, papers are classified according to authors, the research groups the authors belong to, and studies. Different studies are expounded in chronological order. Relevant discussions and future perspectives are given in section 9. Finally, conclusions are drawn in section 10.

## 2. MR fluid and MR actuator

MR fluid is generally made by magnetizable micro-size particles into carrier fluid with stabilizer additives [10]. The most conspicuous feature of MR fluid is that its rheological properties can be changed reversibly in the presence of applied magnetic field [10, 11]. When magnetic field is presented, the magnetizable particles are aligned along the magnetic field and form chain-like structure, restraining movement of the fluid. At this time, the viscosity of MR fluid increases considerably, and MR fluid is in semi-solid state (on state). Upon removal of magnetic field, the semi-solid MR fluid reverses back to its original liquid state (off state). State transformation of MR fluid only occurs within milliseconds. Moreover, when MR fluid becomes semi-solid, the yield stress (the maximum stress that needs to break down the chain-like structure) can be controlled and is determined by applied magnetic field intensity. The controllable and continuous yield stress of MR fluid makes it appropriate for many medical applications. Figure 1 gives the schematic diagram of the working mechanism of MR fluid.

There are four operational modes of MR fluid: flow mode, shear mode, squeeze mode, and pinch mode [12]. In flow mode, also known as valve mode, MR fluid flows between two stationary plates resulted from pressure gradient. In shear mode, also known as clutch mode, MR fluid is located between two plates moving relatively. In squeeze mode, MR fluid flows bi-directionally and is at the same time being compressed or decompressed. In pinch mode, MR fluid flows between two trapezoid plates which are respectively separated by non-magnetic material. Direction of magnetic flux changes, so the slope between pressure and velocity relationship significantly increases compared with that in flow mode. Figure 2 gives the schematic diagram of the four operational modes of MR fluid.

In practical applications, devices that make use of MR fluid are called MR actuators. Generally, MR actuators are mainly divided into three types: MR damper, MR brake, and MR clutch. MR damper is a kind of linear MR actuator that contains damper housing, piston rod, piston head, coil, MR fluid, and gap. MR damper mainly works in flow mode. When piston rod/head move and external electrical current is applied, magnetic flux induced by the magnetic coil wounded on the piston head flows through MR fluid, which increases its yield stress. Consequently, the pressure drop in the length direction of the piston head increases, thus changing the velocity profile of MR fluid in the circular gap. By changing the applied magnetic field, controllable output damping force is generated, which

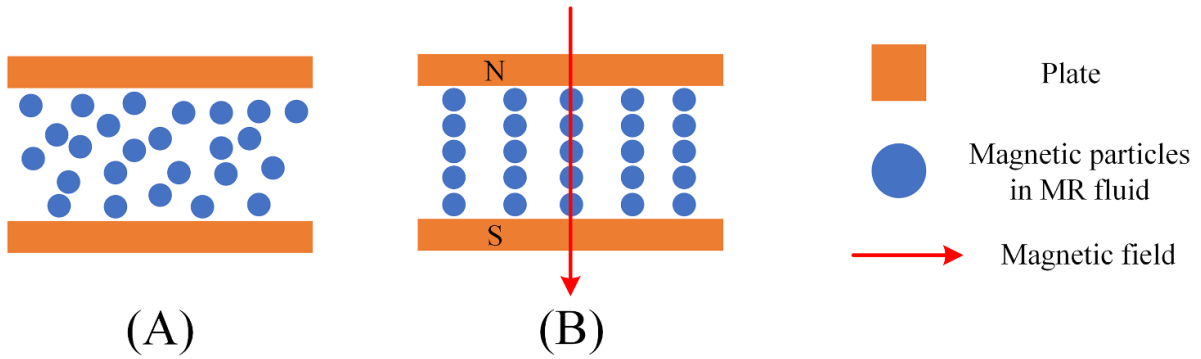


**Figure 1.** Working mechanism of MR fluid. (A) liquid state (off state); (B) semi-solid state (on state).

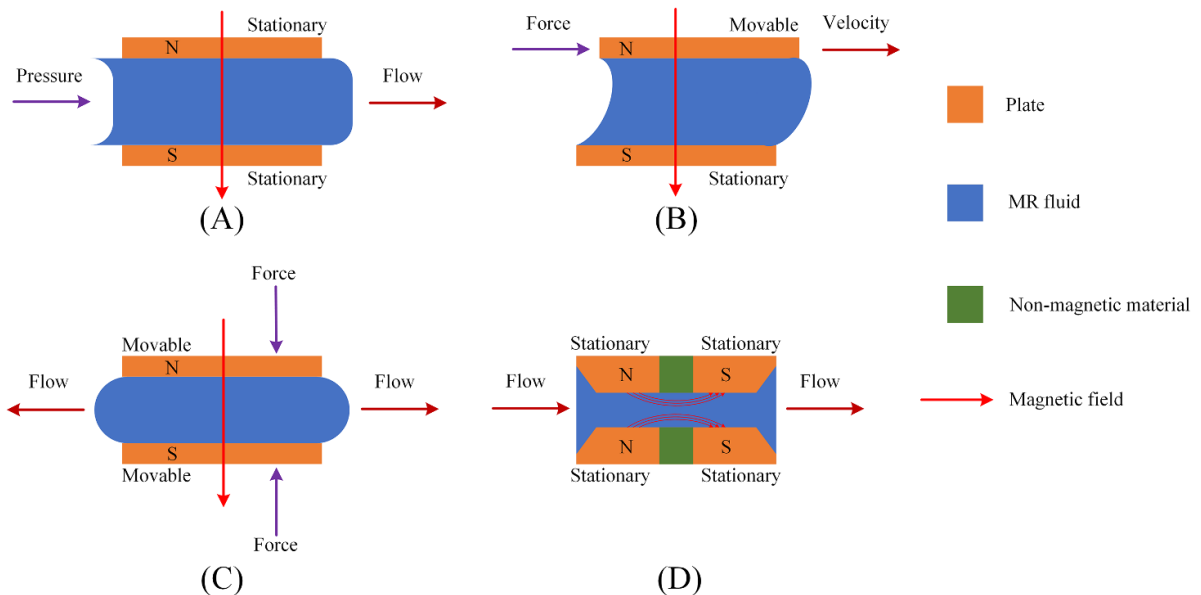


**Figure 2.** Operational modes of MR fluid. (A) Flow mode; (B) shear mode; (C) squeeze mode; (D) pinch mode.

is the major feature of MR damper in practical applications. The basic structures of MR damper include mono-tube type, twin-tube type, and double-ended type [13]. MR brake is a kind of rotary MR actuator that contains rotor, stator, coil, and MR fluid. MR brake mainly works in shear mode. The working principles of MR brake are similar to that of MR damper. Different from MR damper that outputs damping force, MR brake provides resistance damping torque to reduce the angular speed of the rotating shaft immersed in MR fluid. The basic structures of MR brake include drum type, inverted drum type, T-shaped rotor type, disk type, and multiple disk type [14]. MR clutch is the other kind of rotary MR actuator and mainly works in shear mode. It is normally used as controllable auxiliary power transfer device between motor and other supplementary equipment. In some cases, both MR brake and MR clutch can be integrated in one hybrid MR actuator [14–18], and some MR actuators can work in two operational modes [14].

In MR actuators, change of magnetic field intensity is normally realized in two ways: permanent magnet and electromagnet. When mechanically changing the location of

the permanent magnet attached to the moving piston, the magnetization area and the magnet flux dispersion in the MR fluid vary, thus outputting different damping force/torque. Comparatively, with electromagnet, the variation of output damping force/torque is realized by applying different currents to the coil, which can simplify the structural design of MR actuators. These two actuation methods could be used in one device [19].

Before developing MR actuators, modeling methods of MR fluid plays crucial role since precise models can predict the performance of MR actuators. MR fluid models include analytical models and numerical models. Based on the inherent nonlinearity of MR fluid, various analytical models have been summarized in [20, 21]. Also based on the coupling effect of magnetic field and fluid, various numerical models for simulation have been summarized in [22, 23]. After developing MR actuators, implementing appropriate control strategies is also a crucial factor to obtain the desired output responses. Choi *et al* [24] gave a comprehensive summary of various control schemes of MR actuators. Wang and Liao developed control schemes for MR

dampers using neural network [25] and signum function [26].

### 3. Lower limb prosthesis

Generally, lower limb prostheses can be divided into knee (transfemoral) prosthesis for above-knee amputees and ankle (transtibial) prosthesis for below-knee amputees. In terms of actuation mechanisms, there are three types of lower limb prostheses: passive, active, and semi-active types [3, 27]. Passive prostheses are hard to imitate natural gait of walking due to lack of any actuators and external controllers. Although active prostheses can better control the desired walking gait, they consume more energy and may incur instability issues. Semi-active prostheses can provide continuous and controllable damping force/torque using smart materials such as MR fluid, hence offering more natural gait for users. Lower limb prostheses based on MR actuators are also energy efficient, adaptive to various walking speed and different types of activities with fast response time. Therefore, much effort has been devoted into this field and some commercial products have been released to the market. Figure 3 shows some applications of MR fluid in lower limb prosthesis.

#### 3.1. Knee prosthesis

The first knee prosthesis product was the Biedermann Motech Smart Magnetix artificial knee which used a Lord Motion-Master RD-1036 MR damper [28]. It enabled the above knee amputees to walk with natural gait when walking on slopes, up and downstairs, even riding a bicycle. An aluminum housing with standard mounting pylons was used to contain the mechanical assembly. During operation, measured data from rotary position and strain gauge sensors were used to control the MR damper. According to the control signal, the MR damper could respond with resistive force within 30 ms for normal walking. This product was the winner of Smart Structures Product Implementation Award at the 2001 SPIE Industrial and Commercial Applications Conference [29].

Kim *et al* [30] designed an above knee prosthesis with an MR brake. A repetitive controller embedded in a microprocessor combining computed torque and proportional-derivative (CT + PD) control laws was adopted to track repetitive reference profile. Therefore, the root mean square tracking error of knee angle was reduced to 4°. A three-degree-of-freedom (DOF) leg simulator was used to generate various motions to test the above knee prosthesis. Gyro sensor was attached to the thigh to realize real time feedback control so that the prosthesis could be adaptable to walking speeds.

Researchers in Media Lab at Massachusetts Institute of Technology conducted a series of study on MR knee prosthesis. Herr *et al* [31] proposed a user-adaptive MR knee prosthesis actuated by an MR brake. They compared the clinical effects of the MR knee prosthesis with those of conventional non-adaptive knee on four unilateral transfemoral amputees walking at slow, self-selected, and fast speeds. The

results were compared with the gait kinematics of twelve age, weight and height matched normal people. With the user-adaptive control scheme and local mechanical sensing, the user-adaptive knee successfully controlled early stance damping and constrained the maximum swing flexion angle to an acceptable biological limit. This MR knee prosthesis was later patented [32] and became one of the commercial products: Össur Rheo Knee [33]. The detailed compositions [34] and loading mechanisms of MR fluid [35] in Össur Rheo Knee were further investigated. Then, Johansson *et al* [36] further compared the performance of Össur Rheo Knee and hydraulic Otto Bock C-leg with passive Mauch SNS knee. They concluded that Össur Rheo Knee performed better in metabolic rate, smoothness of gait, hip work production, peak hip flexion moment at terminal stance and peak hip power generation at toe-off.

Intelligent bionic leg (IBL) with four-bar link mechanism based on MR damper was proposed Li *et al* and Xie *et al*, which consisted of knee joint, shank, ankle joint, flexible prosthetic foot, and pontes with thigh [37–39]. Modeling of MR damper was investigated, and the fixed position of the MR damper was optimized. The control experiment indicates that IBL could track normal gait of human healthy leg well and has good humanoid characteristics.

Also using the four-bar linkage mechanism, Ochoa-Diaz *et al* [40] developed an above-knee prosthesis with magnetorheological variable-damping (MR damper). This prosthetic knee moved in a polycentric way, which guaranteed stability in stance phase and shortened the prosthesis length during swing phase. Controlled by finite state machine, the performance of the prototype was satisfactory in passive mode (the battery ran out), and could successfully identify heel strike, toe off, mid-swing.

Xu *et al* [41, 42] designed and fabricated a four-bar linkage prosthetic knee based on the magnetorheological effect (FLPKME) and its testing platform. With the mathematical model built and the MR damper simulated, the FLPKME powered by CT + PD control algorithm could track the motions well and imitate the natural motions of a healthy human knee joint. Later, with the upgraded Rayleigh oscillator-based reference angle generator (RORAG) for motion control, the FLPKME could imitate the subject's knee joint's swing angle accurately in real time [43]. Based on FLPKME, Fu *et al* [44] further developed a two-bar linkage magnetorheological damper based lower limb prosthesis (MRLLP). Sliding mode tracking control to track the swing angle of the shank of the MRLLP was shown to be more effective at suppressing hysteresis of MR damper and more robust than CT + PD control algorithm. The experimental results further showed that the controllable joint torque could be successfully generated to control the swing angle of the shank of the MRLLP and to imitate the natural swing of a human knee joint.

Park *et al* [45] proposed a new prosthesis operated in semi-active (driven by MR damper) and active (driven by electronically commutated (EC) motor) modes. Knee joint angle was predicted using polynomial prediction function with statistical method and controlled using CT+ nonlinear PD method. Level ground walking tests showed that the tracking accuracy

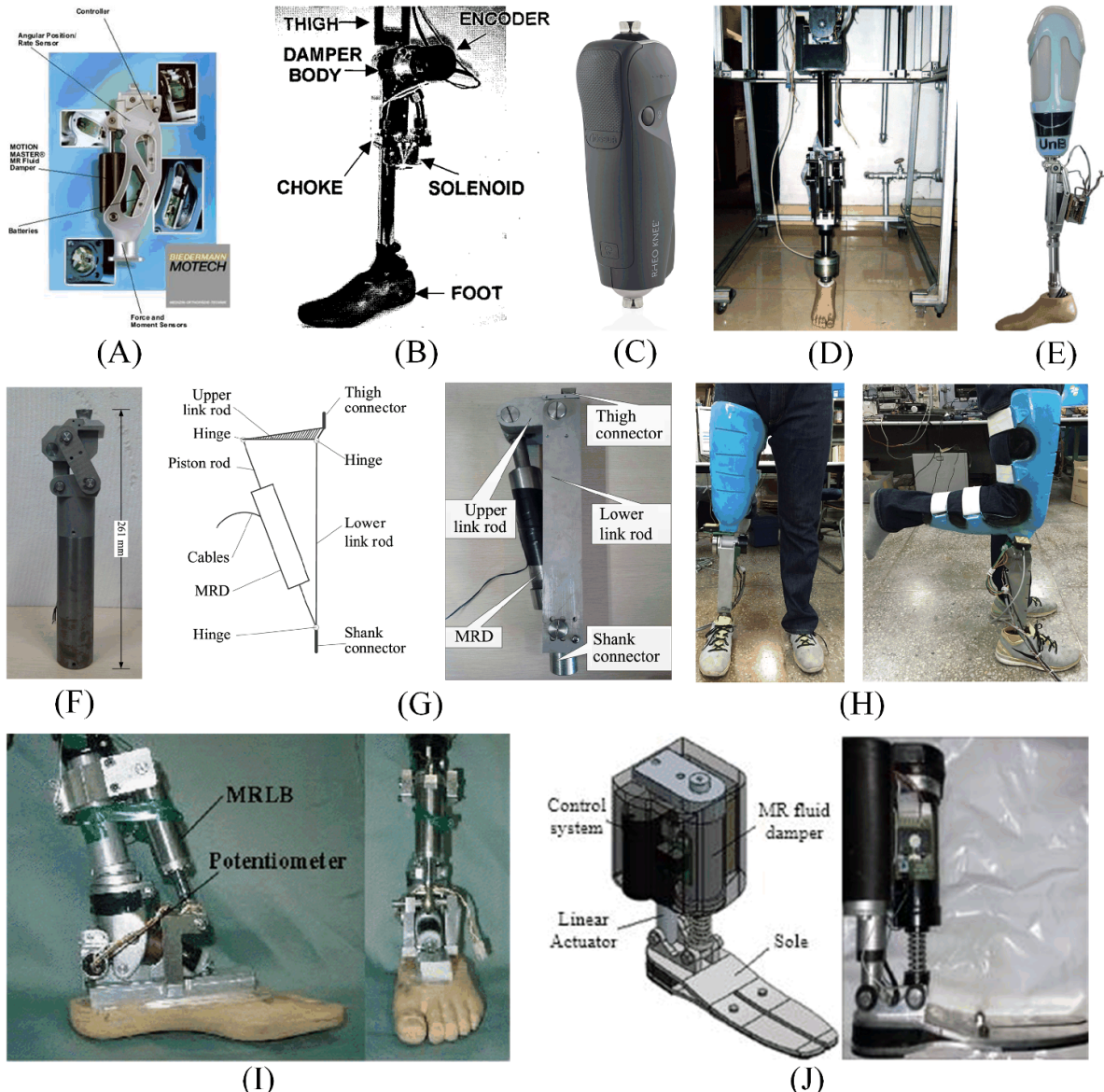


**Figure 3.** Applications of MR fluid in lower limb prostheses. (A) Biedermann Motech Smart Magnetix artificial knee. Reproduced with permission from [29]. (B) the above knee prosthesis by Kim *et al.* © 2001 IEEE. Reprinted, with permission, from [30]. (C) Össur Rheo Knee. Reproduced with permission from [33]. (D) IBL. © 2009 IEEE. Reprinted, with permission, from [37]. (E) the above-knee prosthesis by Ochoa-Diaz *et al.* © 2014 IEEE. Reprinted, with permission, from [40]. (F) FLPKME. Reproduced from [41]. © IOP Publishing Ltd All rights reserved. (G) MRLLP (left: schematic diagram, right: prototype). Reproduced from [44]. © IOP Publishing Ltd All rights reserved. (H) the prosthesis (left: front view, right: side view) by Park *et al.* Reproduced from [45]. © IOP Publishing Ltd All rights reserved. (I) the intelligent prosthetic ankle joint (left: side view, right: front view) by Li *et al.* © IOP Publishing Ltd All rights reserved. © 2006 IEEE. Reprinted, with permission, from [48]. (J) the robotic ankle-foot prosthesis (left: 3D model, right: prototype) by Arteaga *et al.* Reproduced from [49]. CC BY 4.0.

of the actual knee joint angle was high at low walking velocities but was degraded at high walking velocities due to the slow time response of the MR damper. Further studies should be focused on investigation of proper algorithm of gait cycle, optimal design of MR damper to improve the response time, and tests on inclined slope grounds.

Besides the existing work mentioned above, other researchers also performed some preliminary studies on MR actuators to be used in knee prosthesis. Gao *et al* [46] proposed the conceptual design of a self-powered smart prosthetic

knee using an MR damper, a direct current (DC) motor, and springs, in which the optimized MR damper was controlled to hold the springs to store and release mechanical energy. Mousavi *et al* [47] designed and optimized a hybrid T-shaped drum type MR brake with an arc form surface boundary for prosthetic knee. The experimental results showed that the optimized MR brake with 0.69 kg weight generated 38.5 Nm braking torque with controllability and efficiency. Andrade *et al* [17] presented the design, optimization, and torque control of an active magnetorheological knee (AMRK)

actuator (MR brake and MR clutch) for transfemoral prostheses. It could work as a motor, clutch, or brake, reproducing movements of a healthy knee with reduced weight, energy consumption, volume, and aesthetically appropriate structure. Later, study on the energy consumption of AMRK showed that AMRK expended 16.3 J during one gait cycle, which was 1.6 times less than that of the common active knee prosthesis [18].

### 3.2. Ankle prosthesis

Li *et al* [48] designed an intelligent prosthetic ankle joint, in which the MR brake took the place of dorsiflexion. Therefore, the angle displacement and change of center of gravity decreased, which prevented the users from tumbling. Arteaga *et al* [49] proposed a robotic ankle-foot prosthesis with torsion limiting mechanism based on MR damper to emulate the ankle and foot movement in sagittal plane. With the proposed prosthesis, the heel of the prosthesis first contacted the floor, and the MR damper absorbed the impact. Then the motor gave the necessary impulse to complete the next step. Testing results showed that the prototype could replicate the angle and torsion patterns of the human ankle even the stride speed was up to  $2.8 \text{ m s}^{-1}$ .

## 4. Exoskeleton

Besides assisting amputees, MR fluid is also applicable in wearable devices for able-body subjects. Exoskeletons are one of the wearable devices that can assist non-disabled human in different tasks [50]. The significant feature of exoskeletons is that the anatomy of the human limb matches very closely with the kinematic of the devices. They offer robotic force/torque for wearers with user-initiated mobility to reduce or replace the biological joint force/torque when they are walking [2, 51]. Also taking the advantages of controllable and continuous damping force/torque that provides for the joints, exoskeletons based on MR actuators can provide force/strength enhancement, and motion assistance for both upper and lower limbs [52]. Figure 4 shows some applications of MR fluid in exoskeleton.

### 4.1. Exoskeleton for force/strength enhancement

Walsh *et al* [53, 54] firstly presented the application of MR brake in exoskeleton. This load-carrying augmentation exoskeleton used an MR brake similar to the one by Herr and Wilkenfeld [31] in the knee joint. In the MR brake, adjacent blade pairs (one was attached to the thigh and the other one was attached to the lower leg) rotated relative to one another, and there were 77 blades in total. With this design, the maximum braking torque of the knee joint was 60 Nm; 80% of the load was transferred to the ground during the single support phase of walking; and the walking metabolic cost of transport only increased 10% compared with a standard loaded backpack.

### 4.2. Exoskeleton for motion assistance

Baser *et al* [55, 56] designed an ankle joint exoskeleton to assist walking with adjustable stiffness (transmission ratio between the spring and output link) and damping (optimized T-shaped rotor type MR brake). Bench tests of the exoskeleton showed that stable position control could be achieved via open loop control with appropriate stiffness and damping. Later, the similar MR brake prototypes were installed on all joints of a biomimetic compliant exoskeleton robot (BioComEx). Platform tests of BioComEx showed that its trajectory could be successfully controlled using proportional-integral-derivative and derivative (PID + D) control algorithm, though disturbance and oscillations existed. Human tests showed that this configuration could help the impaired leg of the user mimic the motion of his healthy leg with minimal resistance via force feedback impedance control algorithm.

Chen *et al* [57] designed a magnetorheological series elastic actuator (MRSEA) integrated with a compliant torsion spring pack for the knee joints of a lower extremity exoskeleton CUHK-EXO, which could help paraplegic patients stand up, sit down and walk. The MRSEA was used to reduce the mechanical impedance and filter out unwanted collisions of CUHK-EXO. Walking experiments showed that the energy efficiency of CUHK-EXO using MRSEA improved 52.8% during one gait cycle compared with using electric motor.

Véronneau *et al* [58] presented a power distribution system combining MR clutches and hydrostatic transmissions with rolling diaphragms for future applications in exoskeletons. In this system, MR clutches modulated the torque generated from the centralized power source and distribute it to each joint. Due to low reflected inertia, fast response time and low frictional forces, this system could provide high force-bandwidth ( $>40 \text{ Hz}$ ) and good back-drivability ( $\sim 2\%-4\%$ ) with closed-loop control compensation. Using this power distribution system, Khazoom *et al* [59, 60] proposed a multifunctional ankle exoskeleton to assist walking, jumping, and landing, in which a motor was coupled with two MR clutches that modulated the plantar-flexion torque at each ankle. With the state map controller, the MR exoskeleton could produce maximal torque of 90 Nm per ankle with total power of 1.4 kW when jumping. The metabolic cost of the user when walking reduced 5.6% on average. It could also actively brake landing impact and provide multifunctional assistance. Also using this power distribution system, Véronneau *et al* [61, 62] further developed a multifunctional remotely actuated supernumerary robotic arm equipped with a three fingers soft gripper. With torques of 35 Nm for the first two joints and 29 Nm for the third joint, this supernumerary robotic arm could successfully pick fruits and vegetables, paint, hold tools, and play badminton with high speed and smoothness. Also based on this power distribution system, Khazoom *et al* [63] further proposed a supernumerary robotic leg (MR leg) to assist walking with three different gaits: leader-follower gait, double gait, and three-legged gait. The delocalized MR clutches helped to reduce half of the inertial forces transmitted to the user when swinging. The gait cycle of the MR leg was synchronized with the reference trajectory of each ankle's position using an impedance controller.

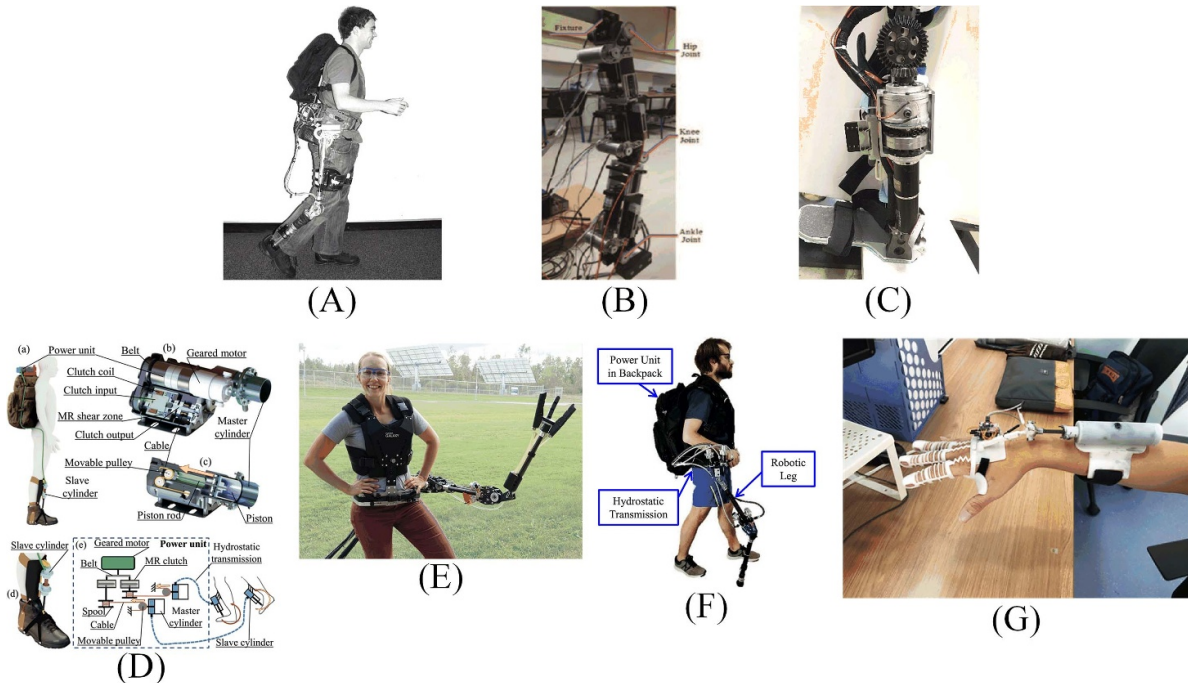


**Figure 4.** Applications of MR fluid in exoskeletons. (A) The load-carrying augmentation exoskeleton by Walsh *et al.* Reproduced with permission from [54]. (B) BioComEx. Reproduced from [56], with permission from Springer Nature. (C) MRSEA. Reproduced from [57]. © IOP Publishing Ltd All rights reserved. (D) the multifunctional ankle exoskeleton by Khazoom *et al.* © 2019 IEEE. Reprinted, with permission, from [59]. (E) the supernumerary robotic arm by Véronneau *et al.* © 2020 IEEE. Reprinted, with permission, from [62]. (F) the supernumerary robotic leg by Khazoom *et al.* © 2020 IEEE. Reprinted, with permission, from [63]. (G) WTSE. © 2019 IEEE. Reprinted, with permission, from [64].

When the user walked at  $1.4 \text{ m s}^{-1}$ , the theoretical maximal average power transmitted to the user within the gait cycle was 84 W, which was four times larger than that of autonomous ankle exoskeleton.

Yi *et al* [64] designed and fabricated a wrist tremor suppression exoskeleton (WTSE) based on MR damper with weight of 262.13 g due to the soft rubber housing. Real-time tremor information acquired by an embedded acquisition platform was used to control the damping force (maximum: 8 N) of the MR damper. The experimental results showed that the amplitude of acceleration and angular velocity of wrist tremor could be reduced 60.39% and 55.07%, respectively. As a following research, Zahedi *et al* [65] proposed a novel soft exoskeleton for tremor suppression (SETS), in which MR fluid was contained in a soft actuator (cylinder-piston damper and elastic fluidic damper). Compared with WTSE, SETS could suppress tremor of joint in three DOFs, was lighter (255 g), and could provide larger damping force (maximum: 11 N). The experimental results showed that the magnitude of acceleration and angular velocity of wrist tremor could be reduced 61.39% and 56.22%, respectively.

## 5. Orthosis

Orthoses are the other kind of wearable anthropomorphic devices that can assist able-body human with limb pathology. Applications of MR fluid in orthoses are generally in two forms: knee assistance devices and ankle foot orthoses

(AFOs). Knee assistance devices are wearable devices to enhance strength and provide desired locomotion for people with walking difficulties [66]. AFOs are wearable medical devices aligned with the ankle and foot of people with paretic ankles to correct orthopedic maladjustment usually caused by stroke, muscular dystrophy, or other neurological injuries [67]. With the help of MR actuators, knee assistance devices can provide proper assisting knee torque as expected thus more natural gait for users; and AFOs can effectively prevent foot drop and absorb shock when foot touches the ground. Figure 5 shows some applications of MR fluid in orthosis.

### 5.1. Knee assistance device

Zite *et al* [68] preliminarily designed an orthopedic knee brace equipped with two MR brakes to provide resistance torque for knee motion. Actuated by two magnets, the resistance torque was 1.8 Nm. This preliminary design was later improved by Ahmadkhanlou *et al* [69], in which the two MR brakes in the knee joints were actuated by currents applied to the solenoids. When the applied current was 4 A, the maximum torque was 6 Nm, with dynamic range of 7.5. However, the device was only tested on a testing machine, and no human test was performed. Large current might lead to issues of safety and practicality, which limited its human use.

Assistive knee braces (AKBs) are a typical kind of knee assistance devices. Chen *et al* [16, 70, 71] developed an AKB equipped with an MR actuator and a DC motor. In active torque mode, the DC motor was on, and the MR actuator

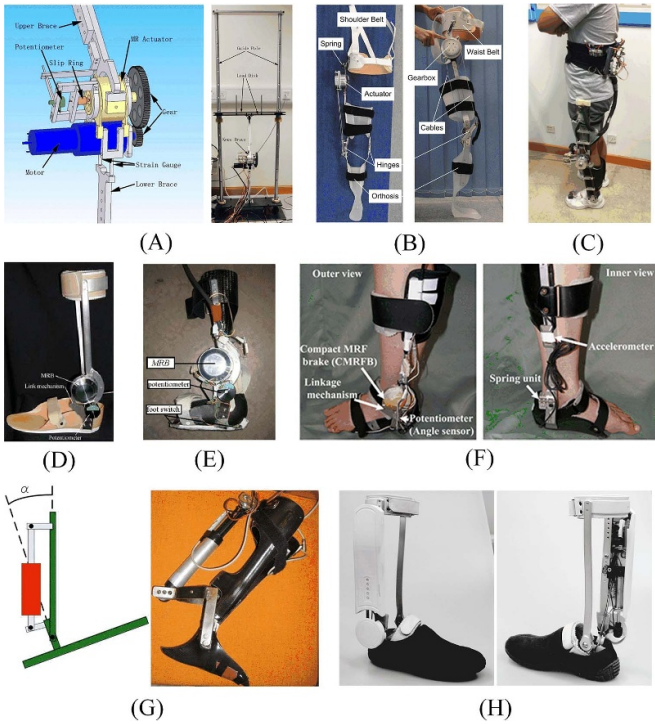


**Figure 5.** Applications of MR fluid in orthoses. (A) the AKB (left: 3D model, right: prototype) by Chen *et al.* © 2011 IEEE. Reprinted, with permission, from [70]. (B) the AKB (left: front view, right: side view) by Guo *et al.* © 2011 IEEE. Reprinted, with permission, from [72]. (C) the AKB with RMRA by Ma *et al.* Reproduced from [75]. © IOP Publishing Ltd All rights reserved. (D) the first generation intelligent AFO by Furusho *et al.* © 2007 IEEE. Reprinted, with permission, from [77]. (E) the second generation intelligent AFO by Tanida *et al.* © 2009 IEEE. Reprinted, with permission, from [78]. (F) the third generation intelligent AFO (left: left view, right: right view) by Kikuchi *et al.* © 2010 IEEE. Reprinted, with permission, from [79]. (G) the AFO (left: schematic diagram, right: prototype) by Svensson *et al.* © 2008 IEEE. Reprinted, with permission, from [80]. (H) SmartAFO (left: right view, right: left view). © 2001 IEEE. Reprinted, with permission, from [30]. © 2008 IEEE.

worked as a clutch to transfer torque from the motor to the leg; while in passive torque mode, the DC motor was off, and the MR actuator worked as a brake to provide controllable torque. With this AKB, the wearer could lift a load of 8 kg when applied current was 1.5 A. It was also safe, energy efficient during normal walking; and had low impedance, better force/torque controllability.

Guo *et al* [15, 72–74] designed a multifunctional rotary actuator that integrated motor and MR fluid into one device. With interior inner coil structure and its main design parameters optimized, this actuator could function as motor, clutch, and brake. Then this actuator was used in an AKB to minimize excessive shifting and improve alignment to the knee joint. Human tests of the first prototype of the AKB when the actuator was off showed that human gait was almost not affected except for knee flexion and rotational motions. In the second prototype, the actuator was moved up to the lateral side of the hip. Human tests showed that walking with the developed knee brace provided minimal hindrance for the wearer.

Ma *et al* [75] designed an AKB equipped with a regenerative magnetorheological actuator (RMRA) for gait assistance in the knee joint. Motor and MR brake in the RMRA worked in parallel, which enabled three braking modes: MR braking, regenerative braking (energy harvesting), and hybrid braking. The MR brake was designed based on optimization to achieve high torque while maintaining light weight and low power consumption. Experimental results showed that the maximal torque was 31.5 Nm when the current was 1.4 A, which satisfied the requirement of gait rehabilitation.

Okui *et al* [76] proposed a knee assistance device actuated by variable viscoelastic joint (antagonized pneumatic muscles) and MR clutch with high back-drivability, which retained structural softness. The feedforward controller was used to control viscosity, elasticity, and angle independently. Structural softness of the proposed system was validated by knee motion experiments (lifting up and down leg motions) with surface electromyography (EMG).

## 5.2. AFO

Furusho *et al* [77] developed the intelligent AFO with a compact MR brake. A compressive force sensor and a bending moment sensor were installed at the shoe sole and shank respectively to obtain timing information to control the MR brake. The testing results showed that the maximum resistive torque was 24 Nm, enabling dorsiflexion maintenance in swing phase and shock absorption at heel strike. Later, Tanida *et al* [78] and Kikuchi *et al* [79] respectively developed the second and third generation intelligent AFO with the sensing and control system improved, and total weight reduced. Experiments on a patient with Guillain-Barre syndrome showed that the gait control of the patient was improved by preventing drop foot in swing phase and forwarding promotion in stance phase.

Svensson *et al* [80] designed an MR damper-based AFO which provided ankle damping during foot down and locking at swing to avoid foot slap and foot drop. Only using the ankle angle, the proposed four-state machine controller enabled the AFO to work independently regardless of gait speed and ground inclinations. Human tests verified the expected behavior in stair gait and level walking, which improved gait comfort in slopes and stairs.

Naito *et al* [81] designed another intelligent AFO based on an MR damper with variable rotational viscosity. In the preliminary experiment, method for detecting walking phase shifts using shank and foot contact information was proposed. In the walking experiment, a hemiplegic subject could keep the ankle dorsiflexed and achieved foot contact by the heel, resulting in appropriate foot/ground clearance during the swing phase.

Adiputra *et al* [82] designed a passive control ankle foot orthosis (PICAFO) using MR brake to prevent foot drop for post-stroke patients. The most distinguishable feature of PICAFO was that the MR brake was controlled based on the EMG bio signal and ankle position. Experimental results showed that the proposed fuzzy logic controller could provide enough voltage and thus resisting torque to prevent foot drop.

Later, the sensor number of PICAFO was further optimized using neural network methods [83].

Ohba *et al* [84] designed an elastic link mechanism (MRLink) where an MR damper was used along with a compression spring, and preliminarily demonstrated its feasibility in upper limb orthosis for sports training, physiotherapy, or motor rehabilitation. Later, this MRLink was integrated into a semiactive AFO (SmartAFO) [85]. This design of SmartAFO could mitigate foot slap and toe drag without adversely affecting push-off or other gait phases. Experiments on a healthy subject showed that SmartAFO could provide controllable braking torque at the heel contact, avoid ankle motion obstruction during the push-off phase, and support toe lift during the swing phase.

Chen *et al* [86] designed and tested a robotic AFO actuated by an SEA and an MR brake for ankle rehabilitation. The proposed robotic AFO could provide dorsiflexion assistance to prevent foot slap at heel contact, toe drag during the swing phase, and plantarflexion assistance for forward propulsion of the body at the push-off stage. The most salient characteristics of the robotic AFO was that it could harvest energy using the motor during walking. During one gait cycle, average power of 0.23 W was harvested, which improved the system efficiency by 8%.

## 6. Rehabilitation device

Rehabilitation devices are developed to enhance muscle strength, flexibility, and proprioception after injury. Different from exoskeletons and orthoses that provide assistance when users are walking, users generally use rehabilitation devices to train specific muscles with scheduled therapies and programs when they are standing still, sitting, or lying down. Rehabilitation devices usually perform repetitive tasks, which enables patients to exercise with different frequencies, durations, and intensities. They also provide different types of exercises (isokinetic, iso-contractile, isometric, isotonic, etc.), and rich stream of information for clinicians and physiotherapists to assist in patients' diagnosis, prognosis, and customized training plan [87]. MR actuators can deliver variable and precisely controlled resistance force/torque; hence they are widely used in rehabilitation devices for both upper and lower limbs. Figure 6 shows some applications of MR fluid in rehabilitation device.

### 6.1. Rehabilitation device for upper limb

Oda *et al* [88] developed an exercise machine using an MR brake with C-type laminated yokes (MEM-MRB) for arm muscle training. MEM-MRB enabled isometric, isokinetic, and iso-contractile exercises for flexion or extension on left or right arm. High speed training over 900°/s of left elbow flexion could be realized, which could not be realized by any other contemporary machines.

Avraam *et al* [89, 90] presented a wrist rehabilitation device based on a T-shape rotor type MR brake. Current control loop (electrical time delay compensation), torque control

loop (current-torque compensation), and motion control loop (motion control of the shaft) were employed so that the device could offer three typical types of muscular exercise: isometric, isotonic, and isokinetic. Comparisons of the proposed device with a commercial one showed that the proposed device was reliable in terms of repeatability.

Kamnik *et al* [91] proposed an exercise device for upper extremity sensory capability augmentation based on a rotational MR actuator. A rotation joint was mounted on the adjustable arm support that provided a controllable resistance during strength training of hand muscles. This device could also provide isometric and isokinetic strength training and was advantageous over electrical motors in terms of power to weight ratio.

Asadi *et al* [92] developed an MR damper-based rehabilitation device for patients to train their damaged hand muscles. The main idea of this device was to generate zones in the device workspace with different resistances to motion (resistance map) through activating the dampers and restricting the motion to the regions determined by the therapists. This method was flexible in defining trainings of damaged muscles. After programmed by physiotherapists, patients could take this device home. The therapist could monitor the progress of patients online and dynamically change their exercises.

Antolini *et al* [93] designed a device for wrist rehabilitation therapy that needed to provide resistive forces against adduction/abduction, flexion/extension of the wrist and pronation/supination of the forearm. This device was coupled to a spherical MR brake which resembled a typical ball joint with three DOFs via linkages so that the virtual center of rotation was at the center of the patient's wrist. Experimental results indicated minimal backlash in the linkages and the device could easily provide controllable resistive forces in its range of motion.

### 6.2. Rehabilitation device for lower limb

Dong *et al* [94–96] designed a rehabilitation device for lower limb muscle strength training of patients with neuromuscular and orthopedic conditions, in which an MR damper was used as variable resistance supply. With optimal design of the MR damper and intelligent supervisory control to regulate the resistive force/torque, the first prototype in the form of a knee brace—variable resistance exercise device, provided both isometric and isokinetic strength training for the knee. With muscle mechanics considered and multi-loop intelligent adaptive control, the second prototype in the form of a rotating joint arm mounted on the adjustable seat—versatile rehabilitation device, precisely monitored the human machine interaction in real-time and provided visual feedback for the patient. Moreover, the automatic adjusting mechanism of the exercise force profile based on artificial intelligence offered flexible and diverse rehabilitation plan for each patient.

Ding *et al* [97] developed the Northeastern University Virtual Ankle and Balance Trainer (NUVABAT) rehabilitation system for (a) training of ankle range of motion in sitting and standing positions, (b) weight shifting and balance training in standing position. This device was with two MR brakes to

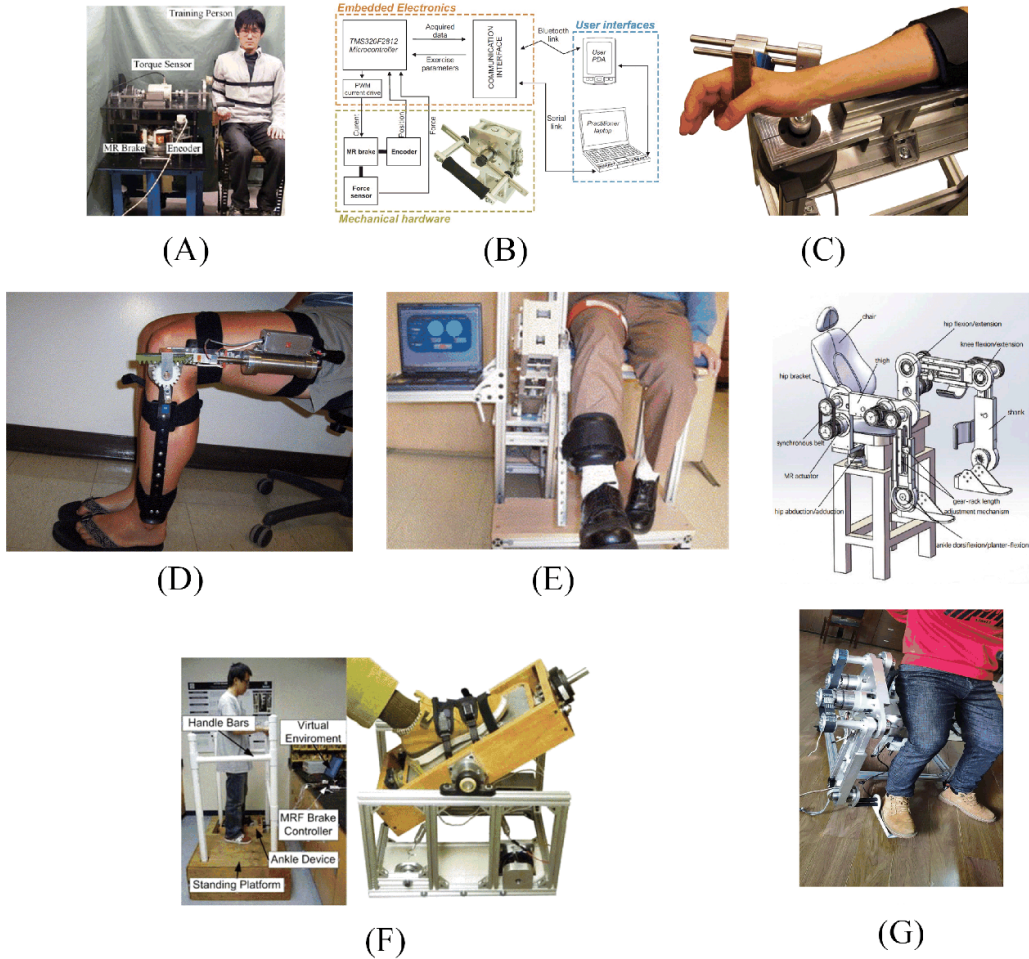


**Figure 6.** Applications of MR fluid in rehabilitation devices. (A) MEM-MRB. © 2009 IEEE. Reprinted, with permission, from [88]. (B) the wrist rehabilitation device by Avraam *et al.* Reproduced with permission from [90]. (C) the exercise device by Kamnik *et al.* © 2010 IEEE. Reprinted, with permission, from [91]. (D) VRED. (D), (E) Reprinted from [94], Copyright (2005), with permission from Elsevier. (E) VRD. (F) NUVABAT (left: testing setup, right: prototype). © 2010 IEEE. Reprinted, with permission, from [97]. (G) the rehabilitation robotic system (upper: 3D model, lower: prototype) by Xu *et al.* © 2019 IEEE. Reprinted, with permission, from [98].

provide adjustable resistance so that it allowed exercising of the ankle motion in two DOFs: plantarflexion/dorsiflexion and inversion/eversion. It was also equipped with a virtual reality interface to run various training programs.

Xu *et al* [98] presented a rehabilitation robotic system equipped with MR actuators to help patients with lower extremity paralysis recover. In robot-active mode, the MR actuator functioned as a clutch to transfer torque to robot joint; while in human-active mode, the MR actuator functioned as a brake to provide resistance to help strengthen muscles. Human intention measured by skin surface EMG determined the working mode, and the device could easily switch between the two modes using adaptive control. Later, based on the same platform, Cheng *et al* [99] used fuzzy logic-based impedance control to study sitting/lying rehabilitation; Xu *et al* [100] investigated the human-machine coupling using AnyBody Modeling System; Shi *et al* [101] studied the trajectory tracking control performance based on neural network.

## 7. Haptic master

With haptic technologies, a robot surgery system can be referred to as a haptic interface with haptic master and slave robot [5]. The surgeon manipulates the haptic master to generate motion control for the slave robot to perform the required surgery. The slave robot sends visual and force data back to the haptic master. The surgeon can see the real-time image of the patient's tissues or organs in the monitor. In the haptic master, the surgeon can feel the resistance force/torque the same with that sensed by the slave robot. Figure 7(A) gives the schematic diagram of robot surgery with haptic force feedback. MR actuators are proper candidates to be built in haptic master to deliver force feedback to the surgeon. Applied current is adjusted according to the force data sensed by the slave robot to control the damping force/torque of the MR actuator, so that the surgeon can feel the force encountered by the slave robot. Figure 8 shows some applications of MR fluid in haptic master.

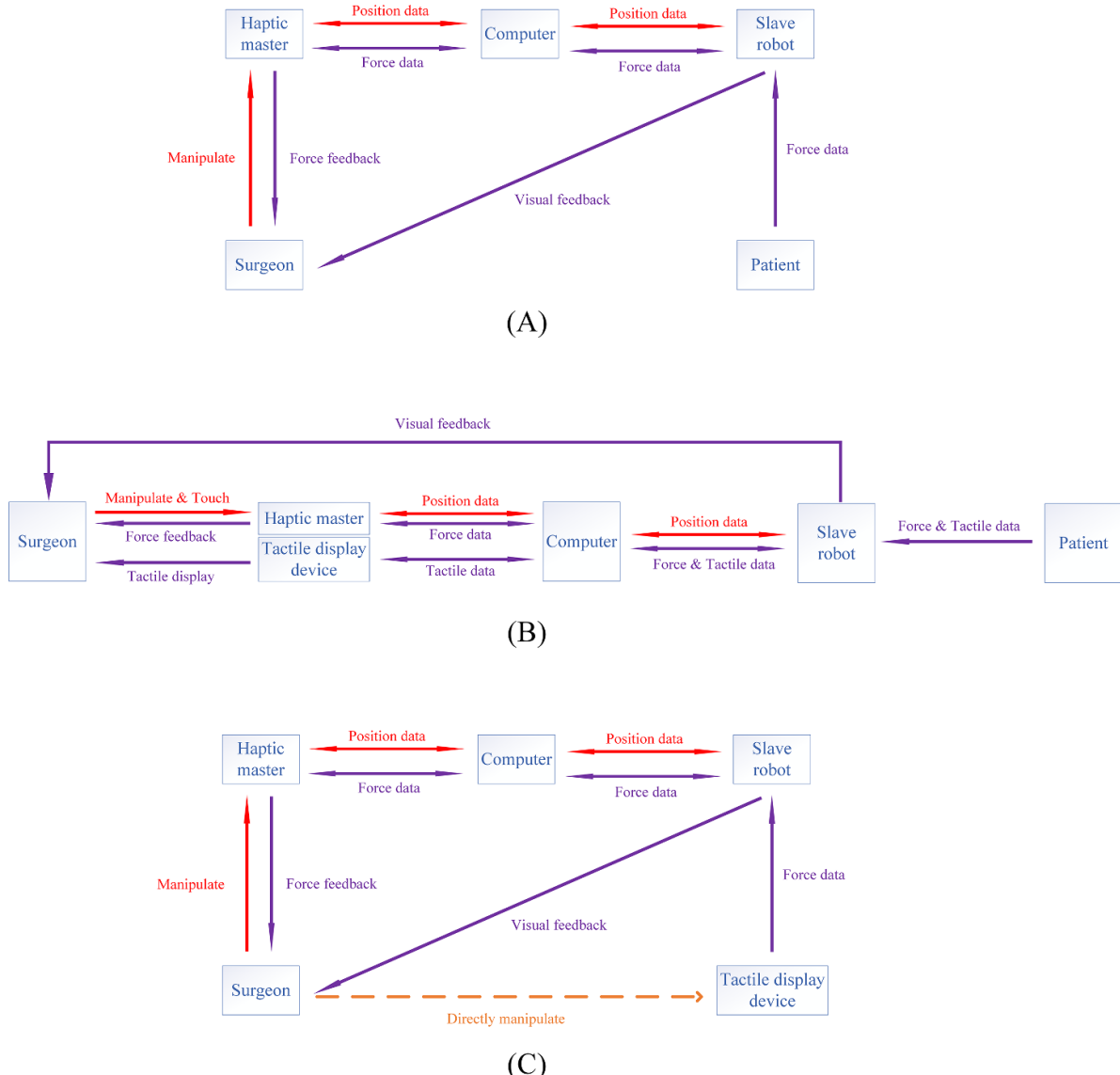


**Figure 7.** Schematic diagram of robot surgery. (A) Haptic master is used to provide force feedback; (B) haptic master and tactile display device are used to provide force and tactile feedback; (C) tactile display device is used to mimic tissues or organs for surgical simulation and training.

Ahmadvand et al [102–104] designed a single-DOF and a two-DOF haptic interfaces for telerobotic surgery. The MR brake joystick was used to command the motion of the end effector and provide resistance force equivalent to that encountered by the probe in the end effector. In the single-DOF interface, the end effector was a flexible rotary probe; while in the two-DOF interface, the probe was connected to a five-bar linkage structure moving in two planar directions. Later, the slave robot was upgraded to a five-DOF system [104, 105]. The experimental results showed that the proposed systems could sense the stiffness of external objects and distinguish hard and soft objects with good stability and transparency.

Senkal et al [106] explored a haptic interface for dental implant surgery. A spherical MR brake with serpentine flux path was designed for six-DOF actuation, with 33% smaller in diameter than the commercial alternatives and 2.7

times more torque at 10.9 Nm. The drilling holes experiment showed that the positioning errors along  $x$  (2.88 mm),  $y$  (1.9 mm), and  $z$  (1.16 mm) axes were on the same order of magnitude as optical tracking systems and other dental robots.

Researchers in Smart Structures and Systems Laboratory at Inha University conducted a series of study on MR-based haptic master for robot surgery. Oh et al [107] designed a four-DOF haptic master (first generation) in which a two-DOF MR bi-directional clutch and a two-DOF MR clutch were integrated. The proposed haptic master was first tested in cyberspace for manipulating virtual objects. The results showed that the desired torque trajectories from cyberspace were well achieved with PID controller. Choi et al [108] added the slave robot and an image processing system for the haptic master. Tumor-cutting experiments showed that the repulsive force at the haptic master matched well with that from the force

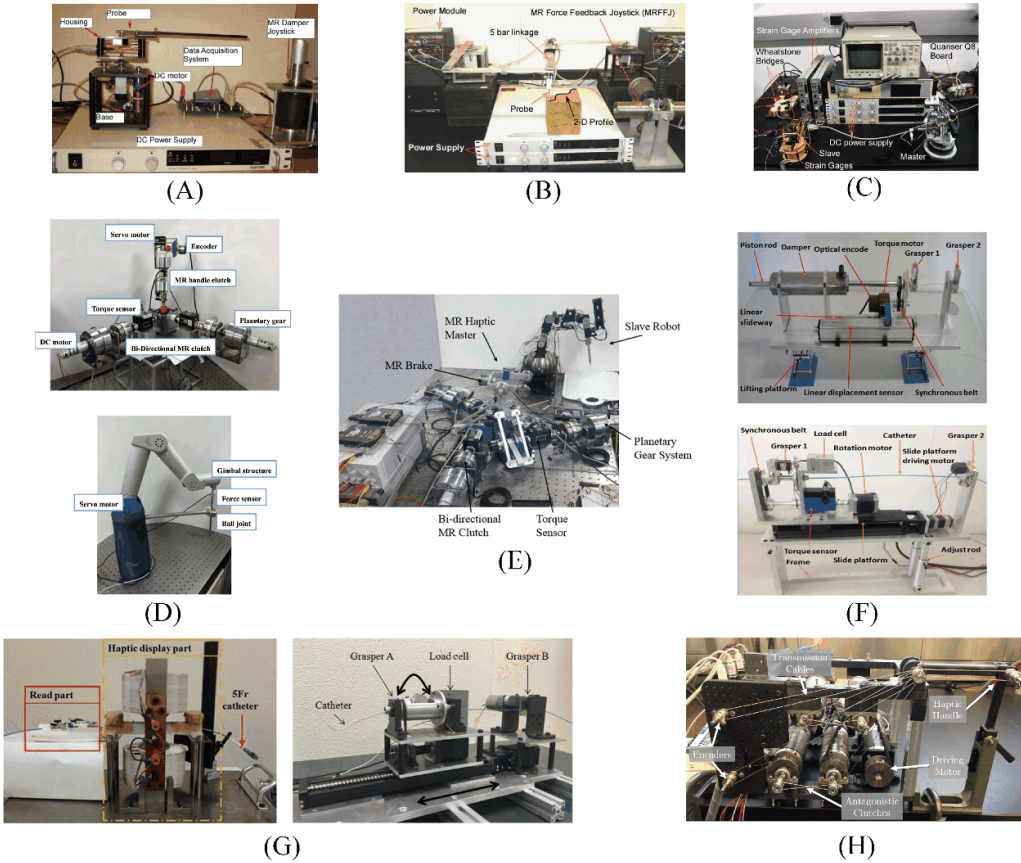


**Figure 8.** Applications of MR fluid in haptic master. (A) The single-DOF haptic interface by Ahmadkhanlou *et al.* (B) the two-DOF haptic interface by Ahmadkhanlou *et al.* (C) the five-DOF haptic interface by Ahmadkhanlou *et al.* (A)–(C) Reproduced with permission from [104]. (D) the four-DOF haptic interface (upper: haptic master, lower: slave robot) by Smart Structures and Systems Laboratory at Inha University. Reproduced from [108]. © IOP Publishing Ltd All rights reserved. (E) the six-DOF haptic interface by Smart Structures and Systems Laboratory at Inha University. Reproduced from [114]. © IOP Publishing Ltd All rights reserved. (F) the RCAS (upper: haptic master, lower: slave catheter manipulator) for VIS. Reproduced from [116], with permission from Springer Nature. (G) the RCAS (left: haptic master, right: slave catheter manipulator) by Guo Lab at Kagawa University. Reproduced from [122], with permission from Springer Nature. © 2019 IEEE. Reprinted, with permission, from [125]. (H) the haptic interface by Najmaei *et al.* © 2015 IEEE. Reprinted, with permission, from [126].

sensor at the slave robot. Image processing also helped distinguish the tumor from the normal organ more clearly. Kim *et al* [109] proposed a reaction force model for incisions, which shortened the training period for robot surgery and could improve operation accuracy. Song *et al* [110] developed a sliding mode controller for this haptic master. The pork-cutting experiments showed that the torque and position trajectories were appropriately achieved by actuating the proposed system. Later, Kang *et al* [111] designed a new six-DOF haptic master (second generation) in which one MR clutch (body segment or lower part) was used to generate repulsive force in three translational directions and one MR brake (wrist segment or upper part) was used to generate repulsive torque for the rotational motion to reflect the slave robot. The overall structure was symmetric so that the translational and rotational motion could be decoupled. Oh *et al* [112] then fabricated the slave robot for the haptic master. Cha *et al* [113] proposed the control strategies with high tracking accuracy for the haptic master. A fuzzy PID feedback controller was used for repulsive force, while a feedforward controller with hysteretic compensator was used for repulsive torque. Hwang *et al* [114] integrated all

the parts of the system and performed tumor-cutting surgery on porcine specimens. The experimental results showed that the surgical accuracy achieved by the haptic feedback control system was much better than that obtained by visual information only.

Yu *et al* [115] conducted preliminary analysis on a robot-assist catheter system (RACS) for vascular interventional surgery (VIS) based on MR damper. The slave manipulator detected the force of catheter when being inserted into the blood vessels, then the master manipulator produced an equal damping force by the MR damper. PID control algorithm with 80.35 mN error was proved effective for online force feedback to reduce the risk of surgery. Later, Guo *et al* [116] developed a multidimensional information monitoring interface to monitor the motion and contact force (measured by sensor array) of the catheter, which effectively enhanced safety during VIS. Guo *et al* [117] analyzed the kinematics performance of the catheter tip and obtained the motion rule of the catheter.

Researchers in Guo Lab at Kagawa University conducted a series of study on RACS for endovascular catheterization based on MR damper. Based on human-centered haptic

interface design concept, Yin *et al* [118, 119] and Song *et al* [120] designed the haptic master of an RACS composed of three parts: magnetic field generation, MR fluid container, and haptic performance calibration mechanism. The performance of the proposed the RACS was tested in terms of magnetic field intensity and distribution, friction, force calibration, force measurement at different insertion and extraction frequencies, hysteresis, physiology hand tremor reduction, transparency, and safety operation consciousness recreation. Song *et al* [121] used virtual reality simulator as the slave side to execute pull, push and twist motions of the virtual cerebral vessel. Experimental results indicated that the proposed RACS could avoid collision and improve safety for endovascular tele-surgery. Zhang *et al* [122] incorporated a collision protection mechanism that could release the catheter quickly when the measured force exceeded a certain threshold to prevent vessel puncture. Yin *et al* [123] developed the slave catheter manipulator and conducted catheter intervention synchronous evaluation and haptic sensation experiments for the proposed master-slave system. Song *et al* [124] implemented a hall sensor-based closed-loop control scheme. Guo *et al* [125] investigated the kinematics of the catheter intervention and introduced ‘pseudo-collision’ and ‘real collision’ to describe the catheter tip–vessel interaction. Experiments showed that the proposed control scheme enabled precise positioning and good transparency.

Najmaei *et al* [126] incorporated a distributed antagonistic configuration of MR clutches into a two-DOF haptic interface for medical percutaneous interventions and soft-tissue palpation. Needle insertion/steering and soft-tissue palpation experiments using phantom and *ex vivo* samples indicated that the proposed MR clutches-based haptic interface was safe, transparent, and stable for force reflection compared with other commercial products.

## 8. Tactile display

Although haptic force feedback can help improve the surgical accuracy, only force feedback sometimes is not enough. Other factors such as compliance, shape, sliding resistance are also contributing to human sensations. Different tissues or organs may deliver the same force feedback, but their sensations to human fingers are totally different. In fact, the word ‘haptic’ refers to force (kinesthetic) feedback and tactile (cutaneous) display [5, 7]. Therefore, tactile display devices are also necessary in robot surgery to enhance sensation experience. Different from normal MR actuators, tactile display devices based on MR fluid are normally made by injecting MR fluid into some carriers (foam, sponge, rubber, etc) and containers. In tactile display devices, MR fluid usually works in squeeze mode. With tactile display, the surgeon can further have the same tactile feelings when touching the tissues or organs of the patient. Tactile display devices are generally in two forms in robot surgery. The first form is that the tactile display device receives the tactile data from the slave robot and provide the same tactile feeling for the surgeon. With force feedback and tactile display, it seems that the surgeon is touching the real

tissues or organs. The second form is that the tactile display device is used to mimic tissues or organs and replace the patient in robot surgery. In this scenario, the slave robot is manipulating the tactile display device, which is often seen in surgical simulation and training. Instead of real patient due to limited resources, the surgeon can perform the surgery or train his/her surgical skills as if he/she is performing surgical manipulation on real patient. Sometimes the surgeon can even directly manipulate the tactile display device with scalpel. Figures 7(B) and (C) gives the schematic diagram of the two forms of tactile display devices in robot surgery. By changing the applied current, tactile display devices based on MR fluid can provide different sensations for human fingers, hence they are widely used in robot surgery. Figure 9 shows some applications of MR fluid in tactile display.

Researchers at University of Pisa firstly proposed the idea of using MR fluid to mimic the compressional compliance of biological tissues for surgical applications and developed some tactile display prototypes. Scilingo *et al* [127] compared the compressional compliance of several MR fluid samples when different magnetic field intensities were applied with specimens of bovine biological tissues. Psychophysical tests on a group of 20 voluntary human subjects showed that the MR fluid samples successfully resembled the perception of liver, spleen, and brain but had unsatisfactory agreement with myocardium, muscle, and lung due to magnetic saturation of MR fluid. Bicchi *et al* [128, 129] and Scilingo *et al* [130, 131] developed two prototypes of tactile display: Pinch Grasp (PG) and Haptic Black Box I (HBB I). PG could squeeze to simulate the viscoelastic behavior of a virtual object when similarly squeezed, hence it was used at the haptic master to remotely probe tissues. HBB I could be used in open surgery simulators and surgical training where the surgeon could interact his/her free hand with virtual replicas of whole organs or complex surgical environments. Later, Rizzo *et al* [132] proposed Haptic Black Box II (HBB II) which could materialize some quasi-3D virtual objects. A prototype with an array of permanent magnets and coils was also developed by Rizzo [19] and showed large improvement in terms of softness and shape reconstruction compared with previous prototypes.

Liu *et al* [133] also conducted preliminary research on MR fluid for tactile display. A single cell MR fluid-based tactile display device equipped with two kinds of electromagnets was designed and tested. When magnetic field was applied, a small bump could be easily felt by dragging a finger over the display surface and the sensed surface profiles changed simultaneously with magnet field intensity.

Lee *et al* [134] further designed a multi-cell tactile display device using MR fluid. In addition to contact force, sensations of contact such as shape, compliance, sliding resistance, and tribological perceptions were examined by measuring normal and shear forces under controlled magnetic fields as well as the effect of arrayed magnetic poles.

Tsujita *et al* [135, 136] designed a haptic interface containing MR fluid to mimic soft tissues and display cutting forces for surgical simulators. A motion table integrated with control scheme was used to help display large deformation of tissues since the elastic region of MR fluid was small. Cutting

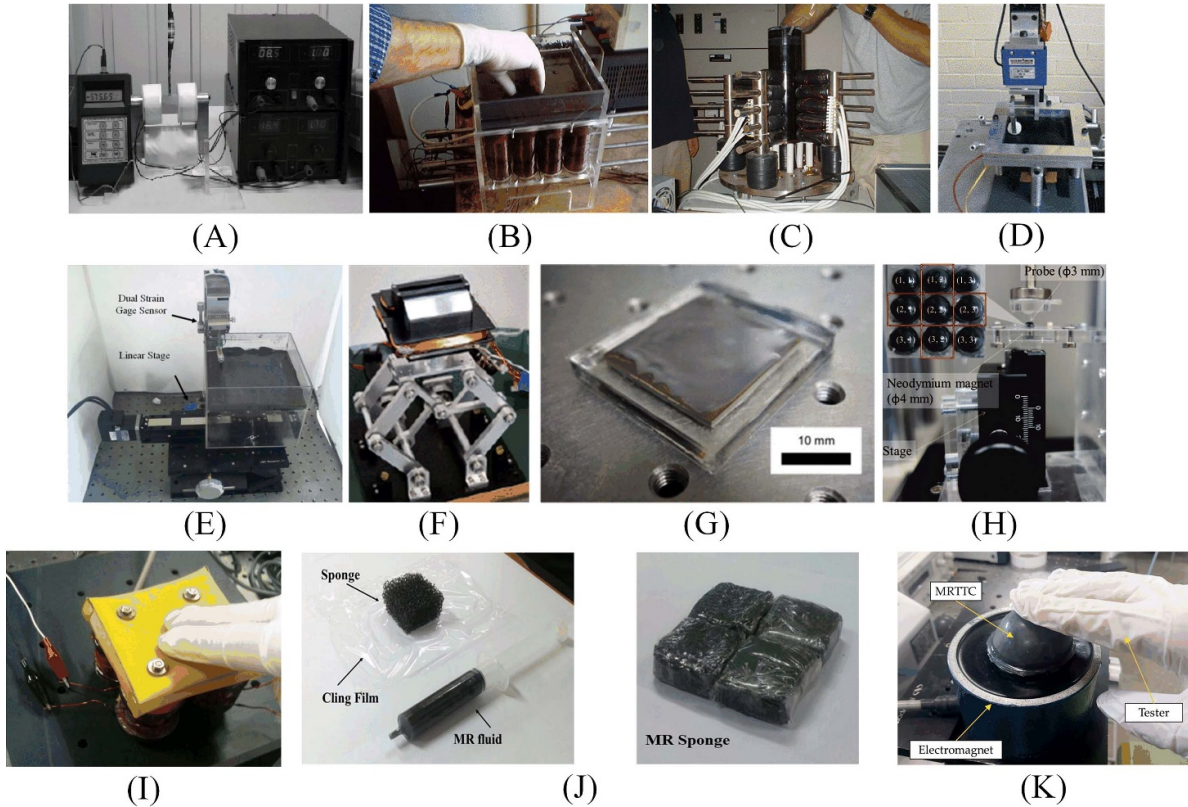


**Figure 9.** Applications of MR fluid in tactile display. (A) PG. © 2007 IEEE. Reprinted, with permission, from [132]. (B) HBB I. (C) HBB II. (B), (C) © 2012 IEEE. Reprinted, with permission, from [19]. (D) the single cell tactile display device by Liu *et al.* Reprinted from [133], Copyright (2005), with permission from Elsevier. (E) the multi-cell tactile display device by Lee *et al.* Reproduced from [134]. CC BY 3.0. (F) the haptic interface to display cutting forces by Tsujita *et al.* © 2012 IEEE. Reprinted, with permission, from [135]. (G) the tactile display device by Ishizuka *et al.* © 2014 IEEE. Reprinted, with permission, from [137]. (H) the tactile display device with nine chambers by Ishizuka *et al.* © 2016 IEEE. Reprinted, with permission, from [139]. (I) the tactile display device by Han *et al.* Reproduced from [141]. © IOP Publishing Ltd All rights reserved. (J) the tactile display device (left: components, right: prototype) by Cha *et al.* Reproduced from [143]. © IOP Publishing Ltd All rights reserved. (K) MRTTC. Reproduced from [146]. CC BY 4.0.

experiments indicated that the interface could exert 2.7 N when the current was 1 A. Therefore, surgeons could feel the resistance force when putting surgical instruments into the fluid, which was conducive to surgical training.

Ishizuka *et al* [137, 138] proposed a tactile display device that could reproduce the spatial stiffness distribution of tissue. The proposed tactile display device could create stiffness values ranging from 200 kPa (normal tissue) to 600 kPa (tumor) with a spatial resolution of less than 5 mm for endoscopic palpation use. In this device, MR fluid was encapsulated in an acrylic chamber covered by a thin flexible membrane. Later, Ishizuka *et al* [139, 140] improved the design of the tactile display by fabricating nine chambers filled with MR fluid on the flexible membrane. The compression experiment revealed that the tactile display device was able to present the stiffness of healthy tissue and tumors by controlling external magnetic field. The five subjects in the sensory experiment were all able to perceive stiff spots smaller than 5 mm when touching the device.

Han *et al* [141] proposed a tactile display device for robot surgery featuring MR fluid based on pin array mechanism. Feedforward control algorithm based on fuzzy logic was used

to obtain the desired palpation force. The actual repulsive forces agreed well with the desired forces with averaged error of less than 1.3%. Participants in the psychophysical test successfully recognized the tactility with a rating value of 3.36/5.

Kim *et al* [142] proposed a tactile display cell for robot surgery using MR fluid and sponge (MR sponge) to realize various magnitudes of force of human-like tissues. The repulsive forces of the MR sponge cell were compared with several animal specimens representing soft and hard tissues of human organ. Cha *et al* [143] later proposed a quasi-static force prediction model for the MR sponge. It was shown that the proposed MR sponge cell could easily produce various levels of the force of human-like tissues, such as the liver and lung of the porcine.

Park *et al* [144, 145] investigated the repulsive force spectrums of MR sponge samples as well as samples made of MR fluid and porous polyurethane foam (PPF). Testing results showed that the MR sponge samples could successfully mimic the viscoelastic properties of pig organs; samples made of MR fluid and PPF had wider controllable range of repulsive force, which were suitable to mimic soft and hard human tissues.

Park and Choi [146] proposed an MR materials-based tactile transfer cell (MRTTC) consisting of MR fluid and magnetorheological elastomer. Measurement results showed that the peak repulsive force at 0.4 A current was 0.959 N, 1.510 N, and 2.783 N at compression depths of 4, 6, and 8 mm, respectively. The repulsive force of MRTTC was also the same as the stress relaxation behavior of human organs. A psychophysical test with 20 volunteers showed that the recognition of repulsive force could reach 4.15/5, and the accuracy of MRTTC was 4.25/5.

## 9. Discussions and future perspectives

### 9.1. Discussions

From the above descriptions, applications of MR fluid in medical devices are summarized in table 1. Meanwhile, structure and key contents of this review article are illustrated in figure 10. MR fluid is the core of this review article, surrounded by a triangle representing its three major actuation forms. Based on these three kinds of MR actuators, six categories of medical applications are expounded as a hexagon. As a special case, MR fluid is directly used in tactile display, expressing as a dashed arrow. Some relevant discussions are given here.

- (a) The large force/torque capacity of MR actuators lies in two aspects. In specific application, the damping force/torque range is big, i.e. large on state force/torque and small off state force/torque, resulting in large dynamic ratio. Among various applications, the ranges of working damping force/torque are also big. For example, the output damping forces of MR dampers range from less than 1 N in haptic master and tactile display to more than 1000 N in lower limb prosthesis and exoskeleton depending on their size and applied electrical current.
- (b) Compared with passive lower limb prostheses, exoskeletons, and orthoses designed with normal mechanical structures and lack of actuation and control strategies, force/torque output of semi-active medical devices based on MR actuators can be better controlled simply by changing the electrical current. Compared with active lower limb prostheses, exoskeletons, and orthoses normally driven by motor, semi-active medical devices based on MR actuators can be stably operated with low power consumption. In fact, as proved by Ahmadkhanlou [102], semi-active devices based on MR actuators are intrinsically stable, which is suitable for medical applications.
- (c) Although there is no specific regulation or standard for using electromagnetic materials in medical devices, relevant safety issues can still be briefly discussed. Generally, MR fluid is made of iron particles, carrier fluid (usually silicon oil), and some additives, which are not erosive and toxic to human. Since the maximum current applied to the coil of the MR actuator is less than 2 A and the electrical resistance of the coil is around several Ohms, the maximum voltage does not exceed 10 V, which is safe for human use. Besides, short time and small amplitude temperature rise does not hurt human because the MR actuators do not contact with human skin in lower limb prosthesis, exoskeleton, orthosis, and rehabilitation devices. Temperature rise in tactile display devices does not influence surgeons as well because surgeons only touch the MR fluid sample, not the coil. Therefore, MR fluid is safe and acceptable for medical devices.
- (d) In the above-mentioned medical devices, MR damper normally works in flow mode to provide damping force, while MR brake and MR clutch usually work in shear mode to provide damping torque. Therefore, MR brake and MR clutch are often used to function as knee and ankle joints to provide rotation torque. Since the rotation speeds of knee and ankle joints during human walking are sometimes not enough for MR brake and MR clutch to generate large torque, additional motor torque is needed, which increases power consumption. Comparatively, MR damper is a good shock absorber in AFO to absorb the large ground reaction force when foot touches the ground. Because MR damper usually output damping force, additional mechanical structures are needed to transfer damping force into damping torque when MR damper is used to perform the function of knee and ankle joints. Although the structure becomes complicated, the rotation torque can be guaranteed since the damping force is already quite large. Additionally, tactile display devices with MR fluid working in squeeze mode have simple and compact structures compared with MR actuators. However, studies and investigations on squeeze mode of MR fluid are immature in current stage, making this kind of device less manageable and practicable. Up till now, MR fluid working in pinch mode has not been applied in medical devices.
- (e) Currently, besides some self-made MR fluid by some researchers, three typical commercial MR fluid products from LORD Corporation are widely used, i.e. MRF-122EG [147], MRF-132DG [148], and MRF-140CG [149]. Their properties are listed in table 2. Yield stresses of the three representative products are respectively given in three values. ‘Yield stress at 50 kA m<sup>-1</sup>’ means yield stress under low magnetic field intensity; ‘Yield stress at 150 kA m<sup>-1</sup>’ means yield stress under high magnetic field intensity; ‘Yield stress at magnetic saturation’ means yield stress under maximum magnetic field intensity. Since the viscosities, densities, and yield stresses gradually increase from MRF-122EG to MRF-140CG, their respective applications in medical devices are different. As can be seen in table 1, MRF-122EG is suitable for tactile display device and haptic master with small damping force/torque. Except for tactile display device, MRF-132DG is applicable to all other categories due to large yield stress range. MRF-140CG is often used in lower limb prosthesis and exoskeleton which need large damping force/torque.
- (f) According to [2, 50], exoskeletons can be generally divided into three categories: force/strength enhancement,

**Table 1.** Summary of applications of MR fluid in medical devices.

Items	Applications	Lower limb prosthesis	Exoskeleton	Orthosis	Rehabilitation device	Haptic master	Tactile display
MR actuators		MR damper	MR brake	MR clutch			
Operation modes of MR fluid			Flow mode	Shear mode			
Advantageous features		Controllable and continuous yield stress	Permanent magnet	Fast state transformation			
Actuation methods		MRF-140CG	MRF-132DG	Electromagnet			
Commercial MR fluid products		MRF-132DG		MRF-132DG	MRF-132DG	MRF-122EG	MRF-122EG
Response time (ms)				30 ~ 250			
Control strategies (including but not limited to)	PID control Sliding mode control	PID control	Fuzzy logic control	Fuzzy logic control	PID control Sliding mode control	Fuzzy logic control	Fuzzy logic control
Force/torque ranges	Adaptive control Force: 0~1500 N Torque: 0~50 Nm	Force: 0~11 N (wrist) 0~1500 N (other)	Force: 0~150 N Torque: 0~20 Nm	Force: 0~100 N Torque: 0~20 Nm	Force: 0~20 N Torque: 0~5 Nm	Force: 0~20 N Torque: 0~5 Nm	Force: 0~5 N
Acting locations of human body	Leg Ankle	Leg Wrist	Leg Ankle	Hand Wrist Arm	Hand	Leg Ankle	Finger



**Figure 10.** Structure and key contents of this review article. Sources of the photos: MR fluid (self-made); MR damper. Reproduced from [46]. © IOP Publishing Ltd All rights reserved. MR brake. Reproduced from [75]. © IOP Publishing Ltd All rights reserved. MR clutch. Reproduced from [16]. © IOP Publishing Ltd All rights reserved. Lower limb prosthesis. Reproduced with permission from [29]. Exoskeleton. Reproduced from [57]. © IOP Publishing Ltd All rights reserved. Orthosis. © 2019 IEEE. Reprinted, with permission, from [85]. Rehabilitation device. © 2019 IEEE. Reprinted, with permission, from [98]. Haptic master. © 2015 IEEE. Reprinted, with permission, from [126]; and Tactile display. Reproduced from [141]. © IOP Publishing Ltd All rights reserved.

**Table 2.** Properties of typical commercial MR fluid products (LORD Corporation).

Items	MR fluid products	MRF-122EG	MRF-132DG	MRF-140CG
Appearance			Dark gray liquid	
Viscosity (Pa·s at 40 °C)		0.042 ± 0.020	0.112 ± 0.020	0.280 ± 0.070
Density (g cm <sup>-3</sup> )		2.28 ~ 2.48	2.95 ~ 3.15	3.54 ~ 3.74
Solids content by weight (%)		72	80.98	85.44
Flash point (°C)			>150	
Operating temperature (°C)			-40 ~ +130	
Yield stress at 50 kA m <sup>-1</sup> (kPa)		11	16	26
Yield stress at 150 kA m <sup>-1</sup> (kPa)		27	39	53
Yield stress at magnetic saturation (kPa) (saturated magnetic field intensity in the right bracket)		34 (410 kA m <sup>-1</sup> )	48 (290 kA m <sup>-1</sup> )	58 (195 kA m <sup>-1</sup> )

motion assistance, and rehabilitation. MR actuators have been applied in exoskeletons for force/strength enhancement and motion assistance but have not been fully utilized in exoskeletons for rehabilitation. The rehabilitation

devices in this review article are different from exoskeletons for rehabilitation. Rehabilitation devices are used to train specific muscles when users are sitting, standing still, or lying; while users wear exoskeletons for

rehabilitation to assist, resist, or perturb their movements to for therapeutic purpose. Exoskeletons for rehabilitation can further train users' nervous system to help them overcome the limitations of disability when they are not wearing the exoskeleton. Some exoskeletons cross over between motion assistance and rehabilitation, such as CUHK EXO that provides both motion assistance [57] and rehabilitation [150].

## 9.2. Future perspectives

- (a) Generally, parts of the MR actuators are made of iron or steel with high density for magnetic induction, which inevitably increases the weight of the system. As for lower limb prosthesis, exoskeleton, and orthosis, other parts should be lightweight to minimize the interference with dynamics of movements and prevent discomfort. Materials with low density and high strength can be used for the mechanical structure, such as carbon fiber and titanium alloy. Other smart materials like shape memory alloys and/or shape memory polymers combining 4D printing technology can also be used to reduce weight and achieve better compliance between human body and the device.
- (b) Up till now, MR actuators applied in lower limb prosthesis, exoskeleton, orthosis, and rehabilitation device are mostly linear and rotary, which poses motion limitations to the human joints. Soft actuators with relatively high human-device interaction and wearing comfort may solve this problem. As mentioned in section 4, soft actuator based on MR fluid has been used in hand exoskeleton to suppress wrist tremor [64, 65]. Recently, soft actuators based on MR fluid have been used in soft robots to increase their autonomy in a scalable and compliant format [151–153]. MR fluid-based soft actuators are also promising to be applied in lower limb prosthesis, exoskeleton, orthosis, and rehabilitation device to bring dexterity and adaptability. Due to their relatively small damping force/torque, they can function as auxiliary actuation strategies in combination with normal MR actuators. Other soft actuation technologies can also be used to form hybrid soft actuators, such as pneumatic artificial muscle, particle jamming, cable, dielectric elastomer actuator, etc.
- (c) Control strategies of MR actuators in medical applications are mainly focused on classical control methods, such as PID control [30, 41, 45, 56, 107, 113, 115], sliding mode control [44, 110], fuzzy logic control [82, 99, 141], adaptive control [31, 96, 98], neural network control [101], etc. More efforts can be devoted into this issue. For example, new customized control schemes that are optimally fitted for particular medical applications should be developed. Moreover, combining several existing control methods may lead to desirable performances, the so-called hybrid control.
- (d) Performance tests of the existing master-slave robot surgery systems based on MR actuator are mainly performed on animal tissues or organs, such as pork, porcine liver, or lung. Similarly, MR fluid-based tactile display devices are also used to mimic animal tissues or organs. These are all *in vitro* tests with simple biological environments. Future research can be focused on *in vivo* tests that incorporate living biological individual with complex inner operation environments. On this occasion, trajectory planning and tracking control of the end effector in the slave robot is crucial to the stable and robust operation of the robot surgery system. MR fluid-based tactile display devices can also be integrated into animal body, so that surgical training can be performed *in vivo* to provide real surgical experience for surgeons.
- (e) Currently, most of the medical devices based on MR fluid are still in developmental stages for research purpose, commercial products are quite few. In the references of this review article, only Biedermann Motech Smart Magnetix artificial knee [28] and Össur Rheo Knee [33] have been released to the market. Limiting factors that prevent lower limb prosthesis, exoskeleton, orthosis, and rehabilitation devices from commercialization mainly include: (a) sedimentation of iron particles of MR fluid that causes performance deterioration; (b) perceivable temperature increments due to long time operation of coil; (c) mechanical friction among different parts of MR actuators; (d) limited number of subjects for testing the prototypes. Reasons why tactile display devices have not been put into market are: (a) possible leakage of MR fluid from its carriers and containers; (b) coupling effect between the carrier and MR fluid that makes the damping performance of the device less controllable and predictable; (c) small amplitude and high sensitivity of repulsive force that requires high precision control. Commercialization of medical devices based on MR fluid can be another possibility that needs collaboration between academia and industry. Different from civil, industrial, and military applications of MR fluid, researchers developing medical products using MR fluid should pay more attention to ergonomic design, device portability, battery life, user training and acclimation, human-machine interaction, system integration, etc.
- (f) Virtual reality has been preliminarily applied in MR fluid-based medical devices. It is adopted as the slave side of the robot surgery system, which enables performance test of the MR fluid-based haptic master without the slave robot [107, 121]. It is also used to provide customized training programs in rehabilitation device [97]. Virtual reality is showing great potential and providing more opportunities. For example, it can simulate various complex motions and scenarios that users wearing lower limb prosthesis, exoskeleton, and orthosis possibly encounter, such as squatting, tumbling, jumping, working on different terrains, etc. This facilitates development for researchers and acclimation for users.
- (g) The kinetic energy of human walking generated from knee or ankle is a great power source that can be harvested for further use. Energy harvesting can be integrated into MR actuator-based medical devices. Although some preliminary investigation has been performed in knee prosthesis [46] and AFO [86], there are still many possibilities in this field. By designing specific mechanical structures

that cooperate with motor and MR actuator, the battery of lower limb prosthesis, exoskeleton, and orthosis can be charged using the harvested energy, so that the whole system can be self-powered or at least more energy efficient. By integrating electromagnetic transduction or other kind of smart materials like piezoelectric material and macro fiber composite, the sensors of lower limb prosthesis, exoskeleton, and orthosis can be powered using the harvested energy, so that the whole system can be self-sensing to become more intelligent or autonomous.

## 10. Conclusions

In the last two decades, MR fluid usually in the form of MR damper, MR brake, and MR clutch, is widely applied in medical field due to fast response, large force/torque capacity, low power consumption, and design simplicity and compactness. Taking the advantages of controllable and continuous yield stress of MR fluid, users wearing lower limb prostheses, exoskeletons, and orthoses can have natural and stable limb motions; users of rehabilitation devices can train their muscles flexibly; robot surgery can have haptic feedback with high transparency and resolution. This review article systematically summarizes the progress of medical applications featuring MR fluid and provides useful information on the potential research opportunities in the future, which is a guide and an impetus for academia and industry to develop more outstanding products.

## Data availability statement

No new data were created or analysed in this study.

## Acknowledgments

This work is supported by the Innovation and Technology Commission (Project No. ITS/367/18) and Research Grants Council (Project No. CUHK 14210019) of Hong Kong Special Administrative Region, China and in part by Hong Kong Centre for Logistics Robotics of InnoHK.

## ORCID iDs

Gaoyu Liu  <https://orcid.org/0000-0001-5136-0733>  
 Fei Gao  <https://orcid.org/0000-0001-9637-6114>  
 Daihua Wang  <https://orcid.org/0003-2786-0046>  
 Wei-Hsin Liao  <https://orcid.org/0000-0001-7221-5906>

## References

- [1] Rabinow J 1948 The magnetic fluid clutch *Trans. Am. Inst. Electr. Eng.* **67** 1308–15
- [2] Kalita B, Narayan J and Dwivedy S K 2021 Development of active lower limb robotic-based orthosis and exoskeleton devices: a systematic review *Int. J. Soc. Robot.* **13** 775–93
- [3] Price M A, Beckerle P and Sup F C 2019 Design optimization in lower limb prostheses: a review *IEEE Trans. Neural Syst. Rehabil. Eng.* **27** 1574–88
- [4] Lanfranco A R, Castellanos A E, Desai J P and Meyers W C 2004 Robotic surgery: a current perspective *Ann. Surg.* **239** 14–21
- [5] Okamura A M 2009 Haptic feedback in robot-assisted minimally invasive surgery *Curr. Opin. Urol.* **19** 102
- [6] Fluit R, Prinsen E C, Wang S and van der Kooij H 2019 A comparison of control strategies in commercial and research knee prostheses *IEEE Trans. Biomed. Eng.* **67** 277–90
- [7] Chouvardas V G, Miliou A N and Hatalis M K 2008 Tactile displays: overview and recent advances *Displays* **29** 185–94
- [8] Oh J-S and Choi S-B 2017 State of the art of medical devices featuring smart electro-rheological and magneto-rheological fluids *J. King Saud Univ. Sci.* **29** 390–400
- [9] Sohn J W, Kim G-W and Choi S-B 2018 A state-of-the-art review on robots and medical devices using smart fluids and shape memory alloys *Appl. Sci.* **8** 1928
- [10] Ashtiani M, Hashemabadi S and Ghaffari A 2015 A review on the magnetorheological fluid preparation and stabilization *J. Magn. Magn. Mater.* **374** 716–30
- [11] De Vicente J, Klingenberg D J and Hidalgo-Alvarez R 2011 Magnetorheological fluids: a review *Soft Matter* **7** 3701–10
- [12] Imaduddin F, Mazlan S A and Zamzuri H 2013 A design and modelling review of rotary magnetorheological damper *Mater. Des.* **51** 575–91
- [13] Zhu X, Jing X and Cheng L 2012 Magnetorheological fluid dampers: a review on structure design and analysis *J. Intell. Mater. Syst. Struct.* **23** 839–73
- [14] Ahamed R, Choi S-B and Ferdaus M M 2018 A state of art on magneto-rheological materials and their potential applications *J. Intell. Mater. Syst. Struct.* **29** 2051–95
- [15] Guo H T and Liao W H 2012 A novel multifunctional rotary actuator with magnetorheological fluid *Smart Mater. Struct.* **21** 065012
- [16] Chen J Z and Liao W H 2010 Design, testing and control of a magnetorheological actuator for assistive knee braces *Smart Mater. Struct.* **19** 035029
- [17] Andrade R, Bento Filho A, Vimieiro C and Pinotti M 2018 Optimal design and torque control of an active magnetorheological prosthetic knee *Smart Mater. Struct.* **27** 105031
- [18] de Andrade R M, Martins J S R, Pinotti M, Filho A B and Vimieiro C B S 2021 Novel active magnetorheological knee prosthesis presents low energy consumption during ground walking *J. Intell. Mater. Syst. Struct.* **32** 1591–603
- [19] Rizzo R 2012 A permanent-magnet exciter for magneto-rheological fluid-based haptic interfaces *IEEE Trans. Magn.* **49** 1390–401
- [20] Wang D H and Liao W H 2011 Magnetorheological fluid dampers: a review of parametric modelling *Smart Mater. Struct.* **20** 023001
- [21] Rossi A, Orsini F, Scorza A, Botta F, Belfiore N P and Sciuto S A 2018 A review on parametric dynamic models of magnetorheological dampers and their characterization methods *Actuators* **7** 16
- [22] Ghaffari A, Hashemabadi S H and Ashtiani M 2015 A review on the simulation and modeling of magnetorheological fluids *J. Intell. Mater. Syst. Struct.* **26** 881–904
- [23] Elsaady W, Oyadiji S O and Nasser A 2020 A review on multi-physics numerical modelling in different applications of magnetorheological fluids *J. Intell. Mater. Syst. Struct.* **31** 1855–97
- [24] Choi S-B, Li W, Yu M, Du H, Fu J and Do P X 2016 State of the art of control schemes for smart systems featuring magneto-rheological materials *Smart Mater. Struct.* **25** 043001

- [25] Wang D H and Liao W H 2005 Modeling and control of magnetorheological fluid dampers using neural networks *Smart Mater. Struct.* **14** 111
- [26] Wang D H and Liao W H 2005 Semiactive controllers for magnetorheological fluid dampers *J. Intell. Mater. Syst. Struct.* **16** 983–93
- [27] Ghillebert J, De Bock S, Flynn L, Geeroms J, Tassignon B, Roelandts B, Lefever D, Vanderborght B, Meeusen R and De Pauw K 2019 Guidelines and recommendations to investigate the efficacy of a lower-limb prosthetic device: a systematic review *IEEE Trans. Med. Robot. Bionics* **1** 279–96
- [28] Carlson J D, Matthis W and Toscano J R 2001 *Smart Structures and Materials 2001: Industrial and Commercial Applications of Smart Structures Technologies* vol 4332 (SPIE) pp 308–16
- [29] Anderson E H and Sater J M 2007 *Industrial and Commercial Applications of Smart Structures Technologies 2007* vol 6527 (SPIE) p 652702
- [30] Kim J-H and Oh J-H 2001 Development of an above knee prosthesis using MR damper and leg simulator *Proc. 2001 ICRA. IEEE Int. Conf. on Robotics and Automation (Seoul, South Korea, 21–26 May 2001)* (IEEE) pp 3686–91
- [31] Herr H and Wilkenfeld A 2003 User-adaptive control of a magnetorheological prosthetic knee *Ind. Robot. Int. J.* **30** 42–55
- [32] Deffenbaugh B W, Herr H M, Pratt G A and Wittig M B 2004 *Electronically controlled prosthetic knee* US6764520B2
- [33] Sigurdsson J 2021 Össur Rheo Knee ([www.ossur.com/en-us/prosthetics/knees/rheo-knee](http://www.ossur.com/en-us/prosthetics/knees/rheo-knee)) (Accessed 12 January 2021)
- [34] Hsu H, Bisbee C R III, Palmer M L, Lukasiewicz R J, Lindsay M W and Prince S W 2006 *Magnetorheological fluid compositions and prosthetic knees utilizing same* US7101487B2
- [35] Bisbee C R III and Hsu H H 2007 *Systems and methods of loading fluid in a prosthetic knee* US7198071B2
- [36] Johansson J L, Sherrill D M, Riley P O, Bonato P and Herr H 2005 A clinical comparison of variable-damping and mechanically passive prosthetic knee devices *Am. J. Phys. Med. Rehabil.* **84** 563–75
- [37] Li F, Xie H, Yuan W and Liu Y 2009 The application research of MR damper in intelligent bionic leg 2009 *Chinese Control and Decision Conf. (Guilin, China, 17–19 June 2009)* (IEEE) pp 1327–31
- [38] Xie H-L, Liang Z-Z, Li F and Guo L-X 2010 The knee joint design and control of above-knee intelligent bionic leg based on magneto-rheological damper *Int. J. Autom. Comput.* **7** 277–82
- [39] Xie H, Liu Z, Yang J, Sheng Z and Xu Z 2016 Modelling of magnetorheological damper for intelligent bionic leg and simulation of knee joint movement control *Int. J. Simul. Model.* **15** 144–56
- [40] Ochoa-Diaz C, Rocha T S, de Levy Oliveira L, Paredes M G, Lima R, Bó A P L and Borges G A 2014 An above-knee prosthesis with magnetorheological variable-damping 5th *IEEE RAS/EMBS Int. Conf. on Biomedical Robotics and Biomechatronics (Sao Paulo, Brazil, 12–15 August 2014)* (IEEE) pp 108–13
- [41] Xu L, Wang D-H, Fu Q, Yuan G and Hu L-Z 2016 A novel four-bar linkage prosthetic knee based on magnetorheological effect: principle, structure, simulation and control *Smart Mater. Struct.* **25** 115007
- [42] Xu L, Wang D-H, Fu Q, Yuan G and Bai -X-X 2019 A novel motion platform system for testing prosthetic knees *Measurement* **146** 139–51
- [43] Xu L and Fu Q 2020 Design and development of a rayleigh oscillator-based reference angle generator for motion control of smart prosthetic knees *IEEE Access* **8** 32421–31
- [44] Fu Q, Wang D-H, Xu L and Yuan G 2017 A magnetorheological damper-based prosthetic knee (MRPK) and sliding mode tracking control method for an MRPK-based lower limb prosthesis *Smart Mater. Struct.* **26** 045030
- [45] Park J, Yoon G-H, Kang J-W and Choi S-B 2016 Design and control of a prosthetic leg for above-knee amputees operated in semi-active and active modes *Smart Mater. Struct.* **25** 085009
- [46] Gao F, Liu Y-N and Liao W-H 2017 Optimal design of a magnetorheological damper used in smart prosthetic knees *Smart Mater. Struct.* **26** 035034
- [47] Mousavi S H and Sayyaadi H 2018 Optimization and testing of a new prototype hybrid MR brake with arc form surface as a prosthetic knee *IEEE/ASME Trans. Mechatron.* **23** 1204–14
- [48] Li C, Tokuda M, Furusho J, Koyanagi K I, Morimoto S, Hashimoto Y, Nakagawa A and Akazawa Y 2006 Research and development of the intelligently-controlled prosthetic ankle joint 2006 *Int. Conf. on Mechatronics and Automation (Luoyang, China, 25–28 June 2006)* (IEEE) pp 1114–9
- [49] Arteaga O, Escorza J, Medina I, Navas R, Amores K and Morales J J 2019 Prototype of robotic ankle-foot prosthesis with active damping using magnetorheological fluids *Int. J. Mech. Eng. Robot. Res.* **8** 753–8
- [50] Young A J and Ferris D P 2016 State of the art and future directions for lower limb robotic exoskeletons *IEEE Trans. Neural Syst. Rehabil. Eng.* **25** 171–82
- [51] Chen B, Ma H, Qin L-Y, Gao F, Chan K-M, Law S-W, Qin L and Liao W-H 2016 Recent developments and challenges of lower extremity exoskeletons *J. Orthopaedic Transl.* **5** 26–37
- [52] Chen B, Zi B, Wang Z, Qin L and Liao W-H 2019 Knee exoskeletons for gait rehabilitation and human performance augmentation: a state-of-the-art *Mech. Mach. Theory* **134** 499–511
- [53] Walsh C J, Paluska D, Pasch K, Grand W, Valiente A and Herr H 2006 Development of a lightweight, underactuated exoskeleton for load-carrying augmentation *Proc. 2006 ICRA. IEEE Int. Conf. on Robotics and Automation (Orlando, FL, USA, 15–19 May 2006)* (IEEE) pp 3485–91
- [54] Walsh C J, Endo K and Herr H 2007 A quasi-passive leg exoskeleton for load-carrying augmentation *Int. J. Hum. Robot.* **4** 487–506
- [55] Baser O and Demiray M A 2017 Selection and implementation of optimal magnetorheological brake design for a variable impedance exoskeleton robot joint *Proc. Inst. Mech. Eng. C* **231** 941–60
- [56] Baser O, Kizilhan H and Kilic E 2020 Employing variable impedance (stiffness/damping) hybrid actuators on lower limb exoskeleton robots for stable and safe walking trajectory tracking *J. Mech. Sci. Technol.* **34** 1–11
- [57] Chen B, Zhao X, Ma H, Qin L and Liao W-H 2017 Design and characterization of a magneto-rheological series elastic actuator for a lower extremity exoskeleton *Smart Mater. Struct.* **26** 105008
- [58] Véronneau C, Bigué J-P L, Lussier-Desbiens A and Plante J-S 2018 A high-bandwidth back-drivable hydrostatic power distribution system for exoskeletons based on magnetorheological clutches *IEEE Robot. Autom. Lett.* **3** 2592–9
- [59] Khazoom C, Véronneau C, Bigué J-P L, Grenier J, Girard A and Plante J-S 2019 Design and control of a multifunctional ankle exoskeleton powered by magnetorheological actuators to assist walking, jumping, and landing *IEEE Robot. Autom. Lett.* **4** 3083–90

- [60] Larose P, Denninger M, Plante J-S, Bigue J-P L and Véronneau C 2020 *Exoskeleton, orthosis, wearable device or mobile robots using magnetorheological fluid clutch apparatus* US20200069441A1
- [61] Véronneau C, Denis J, Lebel L-P, Denninger M, Plante J-S and Girard A 2019 A lightweight force-controllable wearable arm based on magnetorheological-hydrostatic actuators 2019 *Int. Conf. on Robotics and Automation (ICRA)* (Montreal, QC, Canada, 20–24 May 2019) (IEEE) pp 4018–24
- [62] Véronneau C, Denis J, Lebel L-P, Denninger M, Blanchard V, Girard A and Plante J-S 2020 Multifunctional remotely actuated 3-DOF supernumerary robotic arm based on magnetorheological clutches and hydrostatic transmission lines *IEEE Robot. Autom. Lett.* **5** 2546–53
- [63] Khazoom C, Caillouette P, Girard A and Plante J-S 2020 A supernumerary robotic leg powered by magnetorheological actuators to assist human locomotion *IEEE Robot. Autom. Lett.* **5** 5143–50
- [64] Yi A, Zahedi A, Wang Y, Tan U-X and Zhang D 2019 A novel exoskeleton system based on magnetorheological fluid for tremor suppression of wrist joints 2019 *IEEE 16th Int. Conf. on Rehabilitation Robotics (ICORR)* (Toronto, ON, Canada 24–28 June 2019) (IEEE) pp 1115–20
- [65] Zahedi A, Zhang B, Yi A and Zhang D 2021 A soft exoskeleton for tremor suppression equipped with flexible semiactive actuator *Soft Robot.* **8** 432–47
- [66] Zhang L, Liu G, Han B, Wang Z, Li H and Jiao Y 2020 Assistive devices of human knee joint: a review *Robot. Auton. Syst.* **125** 103394
- [67] Chen B, Zi B, Zeng Y, Qin L and Liao W-H 2018 Ankle-foot orthoses for rehabilitation and reducing metabolic cost of walking: possibilities and challenges *Mechatronics* **53** 241–50
- [68] Zite J L, Ahmadkhanlou F, Neelakantan V A and Washington G N 2006 A magnetorheological fluid based orthopedic active knee brace *Smart Structures and Materials 2006: Industrial and Commercial Applications of Smart Structures Technologies San Diego, California, United States 30 March 2006* **6171** (SPIE) p 61710H
- [69] Ahmadkhanlou F, Zite J L and Washington G N 2007 A magnetorheological fluid-based controllable active knee brace *Industrial and Commercial Applications of Smart Structures Technologies 2007 (San Diego, California, United States, 11 April 2007)* **6527** (SPIE) p 65270O
- [70] Chen J and Liao W-H 2009 Design and testing of assistive knee brace with magnetorheological actuator 2008 *IEEE Int. Conf. on Robotics and Biomimetics* (Bangkok, Thailand, 22–25 February 2009) (IEEE) pp 512–7
- [71] Chen J and Liao W-H 2010 Experimental evaluation of an assistive knee brace with magnetorheological actuator 2010 *IEEE Int. Conf. on Robotics and Biomimetics* (Tianjin, China, 14–18 December 2010) (IEEE) pp 1238–43
- [72] Guo H, Hung A S-L, Liao W-H, Fong D T-P and Chan K-M 2011 Gait analysis for designing a new assistive knee brace 2011 *IEEE Int. Conf. on Robotics and Biomimetics* (Karon Beach, Thailand, 7–11 December 2011) (IEEE) pp 1990–5
- [73] Guo H and Liao W-H 2011 Optimization of a multifunctional actuator utilizing magnetorheological fluids 2011 *IEEE/ASME Int. Conf. on Advanced Intelligent Mechatronics (AIM)* (Budapest, Hungary, 3–7 July 2011) (IEEE) pp 67–72
- [74] Hung A S-L, Guo H, Liao W-H, Fong D T-P and Chan K-M 2011 Experimental studies on kinematics and kinetics of walking with an assistive knee brace 2011 *IEEE Int. Conf. on Information and Automation* (Shenzhen, China, 6–8 June 2011) (IEEE) pp 45–50
- [75] Ma H, Chen B, Qin L and Liao W-H 2017 Design and testing of a regenerative magnetorheological actuator for assistive knee braces *Smart Mater. Struct.* **26** 035013
- [76] Okui M, Iikawa S, Yamada Y and Nakamura T 2018 Fundamental characteristic of novel actuation system with variable viscoelastic joints and magneto-rheological clutches for human assistance *J. Intell. Mater. Syst. Struct.* **29** 82–90
- [77] Furusho J, Kikuchi T, Tokuda M, Kakehashi T, Ikeda K, Morimoto S, Hashimoto Y, Tomiyama H, Nakagawa A and Akazawa Y 2007 Development of shear type compact MR brake for the intelligent ankle-foot orthosis and its control; research and development in NEDO for practical application of human support robot 2007 *IEEE 10th Int. Conf. on Rehabilitation Robotics (Noordwijk, Netherlands, 13–15 June 2007)* (IEEE) pp 89–94
- [78] Tanida S, Kikuchi T, Kakehashi T, Otsuki K, Ozawa T, Fujikawa T, Yasuda T, Furusho J, Morimoto S and Hashimoto Y 2009 Intelligently controllable ankle foot orthosis (I-AFO) and its application for a patient of Guillain-Barre syndrome 2009 *IEEE Int. Conf. on Rehabilitation Robotics (Kyoto, Japan, 23–26 June 2009)* (IEEE) pp 857–62
- [79] Kikuchi T, Tanida S, Otsuki K, Yasuda T and Furusho J 2010 Development of third-generation intelligently controllable ankle-foot orthosis with compact MR fluid brake 2010 *IEEE Int. Conf. on Robotics and Automation (Anchorage, AK, USA, 3–7 May 2010)* (IEEE) pp 2209–14
- [80] Svensson W and Holmberg U 2008 Ankle-foot-orthosis control in inclinations and stairs 2008 *IEEE Conf. on Robotics, Automation and Mechatronics (Chengdu, China, 21–24 September 2008)* (IEEE) pp 301–6
- [81] Naito H, Akazawa Y, Tagaya K, Matsumoto T and Tanaka M 2009 An ankle-foot orthosis with a variable-resistance ankle joint using a magnetorheological-fluid rotary damper *J. Biomech. Sci. Eng.* **4** 182–91
- [82] Adiputra D, Ubaidillah U, Mazlan S A, Zamzuri H and Rahman M A A 2016 Fuzzy logic control for ankle foot orthoses equipped with magnetorheological brake *J. Teknol.* **78** 25–32
- [83] Adiputra D, Rahman M A A, Bahiuddin I, Imaduddin F and Nazmi N 2020 Sensor number optimization using neural network for ankle foot orthosis equipped with magnetorheological brake *Open Eng.* **11** 91–101
- [84] Ohba T, Kadone H and Suzuki K 2012 An elastic link mechanism integrated with a magnetorheological fluid for elbow orthotics 2012 *IEEE/RSJ Int. Conf. on Intelligent Robots and Systems (Vilamoura-Algarve, Portugal, 7–12 October 2012)* (IEEE) pp 2789–94
- [85] Oba T, Kadone H, Hassan M and Suzuki K 2019 Robotic ankle–foot orthosis with a variable viscosity link using MR fluid *IEEE/ASME Trans. Mechatron.* **24** 495–504
- [86] Chen B, Zi B, Wang Z, Li Y and Qian J 2021 Development of robotic ankle–foot orthosis with series elastic actuator and magneto-rheological brake *J. Mech. Robot.* **13** 011002
- [87] Khalid Y M, Gouwanda D and Parasuraman S 2015 A review on the mechanical design elements of ankle rehabilitation robot *Proc. Inst. Mech. Eng. H* **229** 452–63
- [88] Oda K, Isozumi S, Ohyama Y, Tamida K, Kikuchi T and Furusho J 2009 Development of isokinetic and iso-contractile exercise machine ‘MEM-MRB’ using MR brake 2009 *IEEE Int. Conf. on Rehabilitation Robotics (Kyoto, Japan, 23–26 June 2009)* (IEEE) pp 6–11
- [89] Avraam M, Horodinca M, Romanescu I and Preumont A 2010 Computer controlled rotational MR-brake for wrist rehabilitation device *J. Intell. Mater. Syst. Struct.* **21** 1543–57

- [90] Avraam M T 2009 MR-fluid Brake Design and Its Application to a Portable Muscular Rehabilitation Device *PhD Thesis* Universite Libre de Bruxelles
- [91] Kamnik R, Perdan J, Bajd T and Munih M 2010 Exercise device for upper-extremity sensory-motor capability augmentation based on magneto-rheological fluid actuator *19th Int. Workshop on Robotics in Alpe-Adria-Danube Region (RAAD 2010)* (Budapest, Hungary, 24–26 June 2010) (IEEE) pp 71–74
- [92] Asadi E, Hoyle A and Arzanpour S 2011 Design of a magnetorheological damper-based haptic interface for rehabilitation applications *J. Intell. Mater. Syst. Struct.* **22** 1269–77
- [93] Antolini M, Köse O and Gurocak H 2013 Haptic device with spherical MR-brake for wrist rehabilitation ASME 2013 *Int. Design Engineering Technical Conf. and Computers and Information in Engineering Conf. (Portland, Oregon, USA, 4–7 August 2013)* (ASME) p V06AT7A003
- [94] Dong S, Lu K-Q, Sun J and Rudolph K 2005 Rehabilitation device with variable resistance and intelligent control *Med. Eng. Phys.* **27** 249–55
- [95] Dong S, Lu K-Q, Sun J and Rudolph K 2006 A prototype rehabilitation device with variable resistance and joint motion control *Med. Eng. Phys.* **28** 348–55
- [96] Dong S, Lu K-Q, Sun J Q and Rudolph K 2006 Adaptive force regulation of muscle strengthening rehabilitation device with magnetorheological fluids *IEEE Trans. Neural Syst. Rehabil. Eng.* **14** 55–63
- [97] Ding Y, Sivak M, Weinberg B, Mavroidis C and Holden M K 2010 Nuvabat: northeastern university virtual ankle and balance trainer *2010 IEEE Haptics Symp. (Waltham, MA, USA, 25–26 March 2010)* (IEEE) pp 509–14
- [98] Xu J, Li Y, Xu L, Peng C, Chen S, Liu J, Xu C, Cheng G, Xu H and Liu Y 2019 A multi-mode rehabilitation robot with magnetorheological actuators based on human motion intention estimation *IEEE Trans. Neural Syst. Rehabil. Eng.* **27** 2216–28
- [99] Cheng G, Xu L, Chen S, Dong L, Xu H and Liu J 2019 Design and control of a sitting/lying style lower limb rehabilitation robot with magnetorheological actuators *2019 IEEE 9th Int. Conf. on Electronics Information and Emergency Communication (ICEIEC) (Beijing, China, 12–14 July 2019)* (IEEE) pp 1–6
- [100] Xu C, Feng B, Xu J, Xu L, Chen S and Wang M 2019 Rehabilitation strategies for the lower limb rehabilitation robot with magnetorheological damper *2019 IEEE 8th Joint Int. Information Technology and Artificial Intelligence Conf. (ITAIC) (Chongqing, China, 24–26 May 2019)* (IEEE) pp 79–84
- [101] Shi J, Xu L, Cheng G, Xu J, Chen S and Liang X 2020 Trajectory tracking control based on RBF neural network of the lower limb rehabilitation robot *2020 IEEE Int. Conf. on Mechatronics and Automation (ICMA) (Beijing, China, 13–16 October 2020)* (IEEE) pp 117–23
- [102] Ahmadkhanlou F, Washington G N and Bechtel S E 2009 Modeling and control of single and two degree of freedom magnetorheological fluid-based haptic systems for telerobotic surgery *J. Intell. Mater. Syst. Struct.* **20** 1171–86
- [103] Ahmadkhanlou F, Washington G N, Wang Y and Bechtel S E 2005 The development of variably compliant haptic systems using magnetorheological fluids *Smart Structures and Materials 2005: Modeling, Signal Processing, and Control (San Diego, California, United States, 19 May 2005)* 5757 (SPIE) pp 491–502
- [104] Ahmadkhanlou F 2008 Design, Modeling and Control of Magnetorheological Fluid-based Force Feedback Dampers for Telerobotic Systems *PhD Thesis* The Ohio State University
- [105] Ahmadkhanlou F, Washington G N and Bechtel S E 2008 The development of a five DOF magnetorheological fluid-based telerobotic haptic system *Modeling, Signal Processing, and Control for Smart Structures 2008 (San Diego, California, United States, 3 April 2008)* **6926** (SPIE) p 692604
- [106] Senkal D 2009 Haptic Surgical Aid System with Magnetorheological Brakes for Dental Implants *Master Thesis* Washington State University
- [107] Oh J-S, Choi S-H and Choi S-B 2014 Design of a 4-DOF MR haptic master for application to robot surgery: virtual environment work *Smart Mater. Struct.* **23** 095032
- [108] Choi S-H, Kim S, Kim P, Park J and Choi S-B 2015 A new visual feedback-based magnetorheological haptic master for robot-assisted minimally invasive surgery *Smart Mater. Struct.* **24** 065015
- [109] Kim P, Kim S, Park Y-D and Choi S-B 2016 Force modeling for incisions into various tissues with MRF haptic master *Smart Mater. Struct.* **25** 035008
- [110] Song B-K, Oh J-S, Kim P, Kim S and Choi S-B 2016 Repulsive torque control of a robot-assisted surgery system using a magnetorheological haptic master *Proc. Inst. Mech. Eng. I* **230** 1116–25
- [111] Kang S-R, Cha S-W, Hwang Y-H, Lee Y-S and Choi S-B 2018 Controllable magnetorheological fluid based actuators for 6-degree-of-freedom haptic master applicable to robot-assisted surgery *Sens. Actuators A* **279** 649–62
- [112] Oh J-S, Sohn J W and Choi S-B 2018 Material characterization of hardening soft sponge featuring MR fluid and application of 6-DOF MR haptic master for robot-assisted surgery *Materials* **11** 1268
- [113] Cha S-W, Kang S-R, Hwang Y-H, Choi S-B, Lee Y-S and Han M-S 2018 Design and control of a parallel mechanism haptic master for robot surgery using magneto-rheological clutches and brakes *J. Intell. Mater. Syst. Struct.* **29** 3829–44
- [114] Hwang Y-H, Kang S-R, Cha S-W and Choi S-B 2019 A robot-assisted cutting surgery of human-like tissues using a haptic master operated by magnetorheological clutches and brakes *Smart Mater. Struct.* **28** 065016
- [115] Yu Y, Guo J, Guo S and Shao L 2015 Modelling and analysis of the damping force for the master manipulator of the robotic catheter system *2015 IEEE Int. Conf. on Mechatronics and Automation (ICMA) (Beijing, China, 2–5 August 2015)* (IEEE) pp 693–7
- [116] Guo J, Guo S and Yu Y 2016 Design and characteristics evaluation of a novel teleoperated robotic catheterization system with force feedback for vascular interventional surgery *Biomed. Microdev.* **18** 1–16
- [117] Guo S, Du W, Guo J and Yu Y 2016 Kinematic analysis of the catheter used in the robot-assisted catheter operating system for vascular interventional surgery *2016 IEEE Int. Conf. on Robotics and Biomimetics (ROBIO) (Qingdao, China, 3–7 December 2016)* (IEEE) pp 1233–8
- [118] Yin X, Guo S, Xiao N, Tamiya T, Hirata H and Ishihara H 2015 Safety operation consciousness realization of a MR fluids-based novel haptic interface for teleoperated catheter minimally invasive neurosurgery *IEEE/ASME Trans. Mechatron.* **21** 1043–54
- [119] Yin X, Guo S, Hirata H and Ishihara H 2016 Design and experimental evaluation of a teleoperated haptic robot-assisted catheter operating system *J. Intell. Mater. Syst. Struct.* **27** 3–16
- [120] Song Y, Guo S, Zhang L and Yin X 2016 MR fluid interface of endovascular catheterization based on haptic sensation *2016 IEEE Int. Conf. on Mechatronics and Automation (Harbin, China, 7–10 August 2016)* (IEEE) pp 454–8
- [121] Song Y, Guo S, Yin X, Zhang L, Wang Y, Hirata H and Ishihara H 2018 Design and performance evaluation of a

- haptic interface based on MR fluids for endovascular tele-surgery *Microsyst. Technol.* **24** 909–18
- [122] Zhang L, Guo S, Yu H, Song Y, Tamiya T, Hirata H and Ishihara H 2018 Design and performance evaluation of collision protection-based safety operation for a haptic robot-assisted catheter operating system *Biomed. Microdev.* **20** 1–14
- [123] Yin X, Guo S and Song Y 2018 Magnetorheological fluids actuated haptic-based teleoperated catheter operating system *Micromachines* **9** 465
- [124] Song Y, Guo S, Yin X, Zhang L, Hirata H, Ishihara H and Tamiya T 2018 Performance evaluation of a robot-assisted catheter operating system with haptic feedback *Biomed. Microdev.* **20** 1–16
- [125] Guo S, Song Y, Yin X, Zhang L, Tamiya T, Hirata H and Ishihara H 2019 A novel robot-assisted endovascular catheterization system with haptic force feedback *IEEE Trans. Robot.* **35** 685–96
- [126] Najmaei N, Asadian A, Kermani M R and Patel R V 2015 Design and performance evaluation of a prototype MRF-based haptic interface for medical applications *IEEE/ASME Trans. Mechatron.* **21** 110–21
- [127] Scilingo E P, Bicchi A, De Rossi D and Scotto A 2000 A magnetorheological fluid as a haptic display to replicate perceived biological tissues compliance *1st Annual Int. IEEE-EMBS Special Topic Conf. on Microtechnologies in Medicine and Biology. Proc. (Cat. No. 00EX451)* (Lyon, France, 12–14 October 2000) (IEEE) pp 229–33
- [128] Bicchi A, Scilingo E P, Sgambelluri N and De Rossi D 2002 *Proc. 2th Int. Conf. Eurohaptics 2002* (EuroHaptics) pp 6–11
- [129] Bicchi A, Raugi M, Rizzo R and Sgambelluri N 2005 Analysis and design of an electromagnetic system for the characterization of magneto-rheological fluids for haptic interfaces *IEEE Trans. Magn.* **41** 1876–9
- [130] Scilingo E P, Sgambelluri N, De Rossi D and Bicchi A 2003 Haptic displays based on magnetorheological fluids: design, realization and psychophysical validation *11th Symp. on Haptic Interfaces for Virtual Environment and Teleoperator Systems 2003. HAPTICS 2003. Proc. (Los Angeles, CA, USA, 22–23 March 2003)* (IEEE) pp 10–15
- [131] Scilingo E P, Sgambelluri N, De Rossi D and Bicchi A 2003 Towards a haptic black box for free-hand softness and shape exploration *2003 IEEE Int. Conf. on Robotics and Automation (Cat. No. 03CH37422)* (Taipei, Taiwan, 14–19 September 2003) (IEEE) pp 2412–7
- [132] Rizzo R, Sgambelluri N, Scilingo E P, Raugi M and Bicchi A 2007 Electromagnetic modeling and design of haptic interface prototypes based on magnetorheological fluids *IEEE Trans. Magn.* **43** 3586–600
- [133] Liu Y, Davidson R, Taylor P, Ngu J and Zarraga J 2005 Single cell magnetorheological fluid based tactile display *Displays* **26** 29–35
- [134] Lee C-H and Jang M-G 2011 Virtual surface characteristics of a tactile display using magneto-rheological fluids *Sensors* **11** 2845–56
- [135] Tsujita T, Ohara M, Sase K, Konno A, Nakayama M, Abe K and Uchiyama M 2012 Development of a haptic interface using MR fluid for displaying cutting forces of soft tissues *2012 IEEE Int. Conf. on Robotics and Automation (Saint Paul, MN, USA, 14–18 May 2012)* (IEEE) pp 1044–9
- [136] Tsujita T, Sase K, Konno A, Nakayama M, Chen X, Abe K and Uchiyama M 2013 Design and evaluation of an encountered-type haptic interface using MR fluid for surgical simulators *Adv. Robot.* **27** 525–40
- [137] Ishizuka H, Lorenzoni N and Miki N 2014 Characterization of tactile display for stiffness distribution using magneto-rheological fluid *2014 Int. Conf. on Electronics Packaging (ICEP) (Toyama, Japan, 23–25 April 2014)* (IEEE) pp 400–4
- [138] Ishizuka H, Lorenzoni N and Miki N 2014 Tactile display for presenting stiffness distribution using magnetorheological fluid *Mech. Eng. J.* **1** FE0034–FE
- [139] Ishizuka H and Miki N 2016 Miniature tactile elements for tactile display with high stiffness resolution with magnetorheological fluid *2016 IEEE 29th Int. Conf. on Micro Electro Mechanical Systems (MEMS) (Shanghai, China, 24–28 January 2016)* (IEEE) pp 1165–8
- [140] Ishizuka H and Miki N 2017 Development of a tactile display with 5 mm resolution using an array of magnetorheological fluid *Jpn. J. Appl. Phys.* **56** 06GN19
- [141] Han Y-M, Oh J-S, Kim J-K and Choi S-B 2014 Design and experimental evaluation of a tactile display featuring magnetorheological fluids *Smart Mater. Struct.* **23** 077001
- [142] Kim S, Kim P, Park C-Y and Choi S-B 2016 A new tactile device using magneto-rheological sponge cells for medical applications: experimental investigation *Sens. Actuators A* **239** 61–69
- [143] Cha S-W, Kang S-R, Hwang Y-H, Oh J-S and Choi S-B 2018 A controllable tactile device for human-like tissue realization using smart magneto-rheological fluids: fabrication and modeling *Smart Mater. Struct.* **27** 065015
- [144] Park Y-J, Yoon J-Y, Lee Y-H and Choi S-B 2019 The repulsive force spectrum of magnetorheological fluids based tactile devices applicable to robot surgery *Curr. Smart Mater.* **4** 75–82
- [145] Park Y-J, Yoon J-Y, Kang B-H, Kim G-W and Choi S-B 2020 A tactile device generating repulsive forces of various human tissues fabricated from magnetic-responsive fluid in porous polyurethane *Materials* **13** 1062
- [146] Park Y-J and Choi S-B 2021 A new tactile transfer cell using magnetorheological materials for robot-assisted minimally invasive surgery *Sensors* **21** 3034
- [147] Auslander E 2021 *LORD Lord technical data—MRF-122EG magneto-rheological fluid ([https://lordfulfillment.com/pdf/44/DS7027\\_MRF-122EGMRFFluid.pdf](https://lordfulfillment.com/pdf/44/DS7027_MRF-122EGMRFFluid.pdf))* (Accessed 28 May 2021)
- [148] Auslander E 2021 *LORD Lord technical data—MRF-132DG magneto-rheological fluid ([https://lordfulfillment.com/pdf/44/DS7015\\_MRF-132DGMRFFluid.pdf](https://lordfulfillment.com/pdf/44/DS7015_MRF-132DGMRFFluid.pdf))* (Accessed 28 May 2021)
- [149] Auslander E 2021 *LORD Lord technical data—MRF-140CG magneto-rheological fluid ([https://lordfulfillment.com/pdf/44/DS7012\\_MRF-140CGMRFFluid.pdf](https://lordfulfillment.com/pdf/44/DS7012_MRF-140CGMRFFluid.pdf))* (Accessed 28 May 2021)
- [150] Chen B, Zhong C-H, Zhao X, Ma H, Guan X, Li X, Liang F-Y, Cheng J C Y, Qin L, Law S-W and Liao W-H 2017 A wearable exoskeleton suit for motion assistance to paralysed patients *J. Orthopaedic Transl.* **11** 7–18
- [151] McDonald K, Rendos A, Woodman S, Brown K A and Ranzani T 2020 Magnetorheological fluid-based flow control for soft robots *Adv. Intell. Syst.* **2** 2000139
- [152] Leps T, Glick P, Ruffatto D III, Parness A, Tolley M and Hartzell C 2020 A low-power, jamming, magnetorheological valve using electropermanent magnets suitable for distributed control in soft robots *Smart Mater. Struct.* **29** 105025
- [153] Hua D, Liu X, Sun S, Sotelo M A, Li Z and Li W 2020 A magnetorheological fluid-filled soft crawling robot with magnetic actuation *IEEE/ASME Trans. Mechatron.* **25** 2700–10